U.S. DEPARTMENT OF COMMERCE
National Technical Information Service

PB-290 859

Laboratory Investigation of the Photooxidation and Catalytic Oxidation of SO2

Calspan Corp, Buffalo, NY

Prepared for

Environmental Sciences Research Lab, Research Triangle Park, NC

Jan 79

United States
Environmental Protection
Agency

Environmental Sciences
Research Laboratory
Research Triangle Park 27711

EPA-600/3-79-006
January 1979

Research and Development

EPA

PB 290859

Laboratory Investigation of the Photooxidation and Catalytic Oxidation of SO_2

FEB 8 1979

REPRODUCED BY
NATIONAL TECHNICAL
INFORMATION SERVICE
U. S. DEPARTMENT OF COMMERCE
SPRINGFIELD, VA. 22161

RESEARCH REPORTING SERIES

Research reports of the Office of Research and Development, U.S. Environmental Protection Agency, have been grouped into nine series. These nine broad categories were established to facilitate further development and application of environmental technology. Elimination of traditional grouping was consciously planned to foster technology transfer and a maximum interface in related fields. The nine series are:

1. Environmental Health Effects Research
2. Environmental Protection Technology
3. Ecological Research
4. Environmental Monitoring
5. Socioeconomic Environmental Studies
6. Scientific and Technical Assessment Reports (STAR)
7. Interagency Energy-Environment Research and Development
8. "Special" Reports
9. Miscellaneous Reports

This report has been assigned to the ECOLOGICAL RESEARCH series. This series describes research on the effects of pollution on humans, plant and animal species, and materials. Problems are assessed for their long- and short-term influences. Investigations include formation, transport, and pathway studies to determine the fate of pollutants and their effects. This work provides the technical basis for setting standards to minimize undesirable changes in living organisms in the aquatic, terrestrial, and atmospheric environments.

This document is available to the public through the National Technical Information Service, Springfield, Virginia 22161.

TECHNICAL REPORT DATA
(Please read Instructions on the reverse before completing)

1. REPORT NO.	2.	3. RECIPIENT'S ACCESSION NO.
EPA-600/3-79-006		PB290859

4. TITLE AND SUBTITLE	5. REPORT DATE
LABORATORY INVESTIGATION OF THE PHOTOOXIDATION AND CATALYTIC OXIDATION OF SO_2	January 1979
	6. PERFORMING ORGANIZATION CODE
7. AUTHOR(S)	8. PERFORMING ORGANIZATION REPORT NO.
R.J. Anderson, R.J. Pilie, E.J. Mack, W.C. Kocmond	NA-5781-M-1
9. PERFORMING ORGANIZATION NAME AND ADDRESS	10. PROGRAM ELEMENT NO.
Calspan Corporation Advances Technology Center 4455 Genesee Street Buffalo, NY 14225	1AA603 AC-13 FY77
	11. CONTRACT/GRANT NO.
	68-02-1785
12. SPONSORING AGENCY NAME AND ADDRESS	13. TYPE OF REPORT AND PERIOD COVERED
Environmental Sciences Research Laboratory - RTP, NC Office of Research and Development U.S. Environmental Protection Agency Research Triangle Park, North Carolina 27711	Final
	14. SPONSORING AGENCY CODE
	EPA/600/09

15. SUPPLEMENTARY NOTES

16. ABSTRACT

The photooxidation of SO_2 in irradiated auto exhaust + SO_2 systems, the catalytic oxidation of SO_2 in the solution droplets of hazes, clouds and fogs containing several concentrations of heavy metals (Mn^{+2} and Fe^{+3}), and the oxidation of SO_2 in irradiated hazes and fogs containing only trace quantities of heavy metals were studied in a 590 m^3 indoor smog chamber. For the irradiated auto exhaust + SO_2 systems, SO_2 oxidation rates as high as 5% hr^{-1} were observed. Primary particulates from auto exhaust produced no discernible effect on SO_2 oxidation. Catalytic oxidation of SO_2 in fogs and hazes was significant under certain conditions, with as much as 6% of the available SO_2 being oxidized in a 30-minute period. No synergistic effect on the rate of SO_2 oxidation was observed from the simultaneous presence of irradiation and a fog or haze.

17. KEY WORDS AND DOCUMENT ANALYSIS

a. DESCRIPTORS	b. IDENTIFIERS/OPEN ENDED TERMS	c. COSATI Field/Group
*Air pollution		13B
*Sulfur dioxide		07B
*Aerosols		07D
*Photochemical reactions		07E
*Catalysis		14B
*Sulfates		
*Test chambers		

18. DISTRIBUTION STATEMENT	19. SECURITY CLASS *(This Report)*	21. NO. OF PAGES
RELEASE TO PUBLIC	UNCLASSIFIED	88
	20. SECURITY CLASS *(This page)*	22. PRICE
	UNCLASSIFIED	A05-A01

EPA Form 2220-1 (9-73)

EPA-600/3-79-006
January 1979

LABORATORY INVESTIGATION OF THE PHOTOOXIDATION AND CATALYTIC OXIDATION OF SO_2

by

R.J. Anderson, R.J. Pilie
E.J. Mack, and W.C. Kocmond

Calspan Corporation
Advanced Technology Center
Buffalo, New York 14225

Contract No. 68-02-1785

Project Officer

B. Dimitriades and J.L. Durham
Atmospheric Chemistry and Physics Division
National Environmental Research Center
Research Triangle Park, N.C. 27711

ENVIRONMENTAL SCIENCES RESEARCH LABORATORY
OFFICE OF RESEARCH AND DEVELOPMENT
U.S. ENVIRONMENTAL PROTECTION AGENCY
RESEARCH TRIANGLE PARK, N.C. 27711

DISCLAIMER

This report has been reviewed by the Environmental Sciences Research Laboratory, U.S. Environmental Protection Agency, and approved for publication. Approval does not signify that the contents necessarily reflect the views and policies of the U.S. Environmental Protection Agency, nor does mention of trade names or commercial products constitute endorsement or recommendation for use.

ABSTRACT

Experimental studies of SO_2 oxidation performed in Calspan's 590 m^3 smog chamber involved the study of the photooxidation of SO_2 in irradiated auto exhaust + SO_2 systems, the catalytic oxidation of SO_2 in the solution droplets of hazes, clouds and fogs containing several concentrations of heavy metals (Mn^{+2} and Fe^{+3}), and SO_2 oxidation in irradiated hazes and fogs containing only trace quantities of heavy metals.

The results of the irradiated auto exhaust + SO_2 systems revealed that the use of leaded fuels produced increased numbers of primary particulates and reduced visibilities as compared to unleaded fuels. Systems containing high hydrocarbon concentrations (HC/NO_x >50/1) revealed an apparent enhanced rate of SO_2 photooxidation ($\sim$5% hr^{-1}) during about the first two hours of the irradiation. Following this initial period of enhanced SO_2 photooxidation, little or no further SO_2 conversion was observed. The primary particulates of the auto exhaust produced no discernible effect on the oxidation of SO_2.

The catalytic oxidation of SO_2 in fogs and hazes was found to be significant under certain conditions. In nonirradiated dense hazes (b_{scat} on the order of $10^{-2}m^{-1}$) containing about 1 $\mu g/m^3$ each of Mn^{+2} and Fe^{+3}, as much as 80 $\mu g/m^3$ of sulfate was formed within 30 minutes after the introduction of SO_2. This quantity of sulfate corresponds to the oxidation of almost 3% of the available SO_2 (0.75 ppm). Fog water samples ($\sim$10 ml) from simulated natural fogs (LWC $\sim$0.3 g/m^3) contained about 360 $\mu g/ml$ of sulfate for measured concentrations of Mn^{+2} and Fe^{+3} of about 2 $\mu g/ml$ each and an ambient SO_2 concentration of about 0.4 ppm. This sulfate concentration corresponds to over 6% conversion of the available SO_2.

No synergistic effect on the rate of SO_2 oxidation was observed from the simultaneous presence of irradiation and a fog or haze. The measured

rate of SO_2 oxidation in irradiated hazes (b_{scat} <3 x 10^{-4} m^{-1}) containing only trace concentrations of heavy metals agreed well with the observed rate of SO_2 photooxidation in irradiated clean air systems (~0.2% hr^{-1}). In subsequent irradiated fog experiments also containing only trace concentrations of heavy metals, the observed sulfate formation appeared to be consistent with that expected from summing the sulfate formation found in similar nonirradiated fogs with that measured in irradiated clean air experiments.

This report was submitted in fulfillment of 68-02-1785 by Calspan Corporation under the sponsorship of the U.S. Environmental Protection Agency. This report covers a period from July 1, 1975 to January 1, 1978, and work was completed as of January 30, 1978.

CONTENTS

Abstract....iii
Figures....vi
Tables....vii
Abbreviations and Symbols....viii
Acknowledgments....ix

1. Introduction....1
2. Conclusions....4
3. Recommendations....8
4. Experimental Facilities....10
5. Aerosol Sampling and Sulfate Analysis....15
6. SO_2 Photooxidation in HC+NO_x+SO_2 Systems....19
   - The HC+NO_x+SO_2 Systems....19
   - Auto Exhaust Experiments....25
7. Catalytic SO_2 Oxidation in Clouds, Fogs and Hazes....34
   - Haze and Fog Generation....36
   - Haze Experiments....37
     - Nonirradiated Haze Experiments....37
     - Irradiated Haze Experiments....46
     - Discussion of Results....49
   - In-Fog Experiments....51
     - Results....61
     - Discussion of Results....67

References....70
Appendix A Microphysical Characteristics of Selected Laboratory Fogs..73

FIGURES

Number		Page
1	Cut-Away View of Calspan Environmental Simulation Facility.....	11
2	Inside View of Calspan's 600 m^3 Photochemical Aerosol Chamber.....	12
3	Schematic Drawing of Heated Sampling Inlet.....	18
4	Sulfate Concentrations Versus Time for the Indicated Irradiated Auto Exhaust + SO_2 Experiments.....	29
5	Rate of SO_2 Oxidation Versus Time for Indicated Irradiated Auto Exhaust + SO_2 Experiments.....	30
6	Rate of SO_2 Oxidation Versus Time for the Indicated Irradiated Auto Exhaust + SO_2 Experiments.....	31
7	Rate of SO_2 Oxidation Versus Time for the Irradiated Auto Exhaust + SO_2 Experiments.....	32
8	Parameters for Hazes Nebulized from Aqueous Solutions Containing 10^{-3}M and 10^{-2}M NaCl.....	40
9	Cumulative Size Distributions for Hazes Nebulized from Aqueous Solutions Containing 10^{-3}M and 10^{-2}M NaCl for Specified Relative Humidities.....	41
10	Typical Diffusion Chamber Data Showing CCN Concentration for 0.3% Supersaturation from Aerosols Produced by the Nebulization of an Aqueous Solution Containing 10^{-3}M and 10^{-2}M NaCl.....	44
11	Microphysical Characteristics of Fog #100/1 as Functions of Time...	58
12	Dependence of Sulfate Content of Fog Water on SO_2 Concentration and Heavy Metals.....	64

TABLES

Number		Page
1	Complete Log of Calspan Smog Chamber Experiments	20
2	Summary of Chemistry Data from HC+NO_x and HC+NO_x+SO_2 Irradiations	23
3	Summary of Aerosol Data from HC+NO_x and HC+NO_x+SO_2	24
4	Log of Auto Exhaust Experiments	26
5	Auto Exhaust Experiments - Chemistry Data	28
6	Haze Experiments	39
7	Sulfate Formation in Pre-fog Hazes Indicating Dependence on Heavy Metals	45
8	Irradiated Haze Experiments	47
9	In-Fog Experiments	52
10	Irradiated In-Fog Experiments	54
11	Mean Fog Microphysical Properties	59
12	Chemistry of In-Fog Experiments	62

ABBREVIATIONS AND SYMBOLS

ABBREVIATIONS

AE	-- auto exhaust
CID	-- cubic inch displacement
CCN	-- cloud condensation nuclei
CYCLO	-- cyclohexene
EAA	-- electrical aerosol analyzer
HC	-- hydrocarbon
LWC	-- liquid water content
N_{max}	-- maximum observed number of aitken nuclei
PROP	-- propylene
RH	-- relative humidity
R_{SO_2}	-- rate of oxidation of sulfur dioxide
r_x	-- reaction
w/	-- with
w/o	-- without
XRF	-- x-ray fluorescence

ACKNOWLEDGMENT

The authors wish to acknowledge the many helpful discussions with and the support of Dr. Jack L. Durham, Technical Project Monitor. Dr. Richard Keppler, Director of ORD in EPA Region 1, also provided information and guidance in the performance of the project. Appreciation is expressed for the X-ray fluorescence analysis provided by R. B. Kellogg and J. M. Lang of Northrop Services, Inc. and ion chromatography performed by Melville Richards of Northrop Services, Inc. and Kevin Peterson of the Environmental Protection Agency at Research Triangle Park, North Carolina. Many individuals at Calspan unselfishly provided time and effort during the performance of this project. They include Thomas Niziol, John Michalovic, C. William Rogers, Dr. Ulrich Katz, and Dr. John Yang. The text was typed by Mrs. Marilyn T. Handley.

SECTION 1
INTRODUCTION

Atmospheric gas to particulate conversion processes are widely recognized as complicating factors in the development of air quality criteria and associated emission control strategies. The ubiquitous presence of SO_2 in the urban atmosphere together with the effects of sulfuric acid and sulfate aerosols make the understanding of SO_2 oxidation in the ambient atmosphere especially important. As a part of a broad base program under the auspices of the EPA, Calspan performed smog chamber simulation studies to assess the SO_2 oxidation rates and mechanisms in varying ambient environments. Early in the program, emphasis was placed on investigating chemical and aerosol behavior under homogeneous photooxidation conditions. In the latter stages of the program, experiments were directed toward studies of solution droplet catalytic effects on SO_2 oxidation as might be expected under in-cloud transformation and power plant plume conditions. In addition, considerable effort was expended to develop and refine reliable sulfate sampling and analysis procedures.

The SO_2 photooxidation rate in clean filtered air as determined by smog chamber (Kocmond and Yang, 1975) and flow reactor (Kasahara and Takahashi, 1976) measurements appears to be about a few tenths of a percent per hour under noontime sunlight irradiation at middle latitudes. In polluted atmospheres with the presence of nitrogen oxides and reactive hydrocarbons, the homogeneous photooxidation process may, however, result in SO_2 to aerosol conversion rates of several percent per hour (Hidy and Burton, 1975). A mechanism of aerosol formation by OH radical reaction with SO_2 has been proposed by Wood, Castleman and Tang (1975). Calvert and McQuigg (1975) demonstrated by computer simulation that enhanced photooxidation of SO_2 in

nitrogen oxide and hydrocarbon polluted atmospheres would be consistent with such a proposed mechanism. The formation of intermediate molecular complexes of SO_2 with hydrocarbon and nitrogen oxides contaminants has been proposed as another possible mechanism (Richards, Fox, and Reist, 1976) giving rise to enhanced SO_2 oxidation via homogeneous photochemical processes. In view of the current lack of understanding of the complex mechanisms involved in SO_2 photooxidation under polluted urban atmospheres, smog chamber determinations of the oxidation rate under a variety of contaminant conditions are needed.

In-cloud transformation of SO_2 to sulfate is considered as an important route responsible for sulfur balance in the environment. One likely transport mechanism of sulfur pollutants from the atmosphere to the earth is the scavenging of SO_2 during cloud droplet formation and subsequent precipitation. During nonprecipitation events, the cloud droplets form aloft and evaporate prior to reaching the earth. As a result, the in-cloud SO_2 to sulfate transformation preceding droplet evaporation produces residual sulfate aerosols in the atmosphere. Junge and Ryan (1958) were among the first to investigate the rate of SO_2 oxidation in dilute aqueous solutions and found rapid conversion in the presence of trace metal ions which appeared to serve as catalysts. Radke (1970) apparently observed residual sulfate aerosols in conjunction with wave clouds over Mt. Ranier, Washington. In several instances he noted cloud condensation nuclei concentrations in the air leaving the wave clouds to be significantly greater than those entering the cloud.

Another likely environment favorable to aqueous droplet SO_2 to sulfate conversion is that existing within the power plant stack emission plume. A stack plume from a combustion process is typically a continuous point source of hot gases rising vertically due to a buoyancy effect. The rising air mass is cooled due to the expansion and mixing with cold ambient air, which under proper conditions results in condensation. The droplets thus formed are transported within the plume and present a reaction medium conducive to SO_2 oxidation. To date, there are no convincing atmospheric studies that support this mechanism.

Experiments were performed in the Calspan chamber to compile SO_2 oxidation kinetic data under a wide range of environmental conditions likely to be encountered in the real atmosphere. In order to ascertain the effects of individual environmental variables on SO_2 oxidation, initial efforts emphasized the establishment of base line kinetic data under clean air conditions for both the homogeneous gas phase and the in-cloud transformation processes. A major effort was expended in refining procedures for collection of sulfate aerosols free of artifact conversion effects and for analysis of sulfate at the low concentration ranges often observed in clean air.

This report covers the entire 30 months of the current program. Conclusions drawn during the program are presented in Section 2 and recommendations for future related work are given in Section 3. A brief description of experimental facilities is provided in Section 4, while a discussion of aerosol sampling techniques and sulfate analysis procedures is presented in Section 5. Data summaries in Section 6 cover the series of experiments on SO_2 photooxidation in the presence of propylene and NO_x and in the presence of auto exhaust. In Section 7, the results of the investigations of the oxidation of SO_2 in haze and cloud droplets are presented. Literature references are presented in Section 8.

SECTION 2
CONCLUSIONS

Three extensive sets of experiments were performed on this program to investigate oxidation processes of SO_2 and associated changes in aerosol characteristics in the atmosphere. These included photooxidation in $HC+NO_x+SO_2$ systems (primarily auto exhaust + SO_2 systems), catalytic oxidation in haze and fog aerosols, and combined catalytic and photooxidation in haze and fog systems.

Early experiments demonstrated that conventional methods for sample collection and chemical analysis were not adequate for direct, quantitative measurements of sulfate production under the required experimental conditions. In related internally-supported programs, therefore, two new sampling systems were developed at Calspan for providing samples that could be analyzed with the most modern and sophisticated analytical equipment available at the EPA's Research Triangle Park (RTP).

One sampling system consisted of a filter holder with a heated air inlet that evaporates all liquid water of wet aerosols before collection on teflon fluoropore membrane filters. This system minimized artifact sulfate formation stimulated by wet catalytic processes on the filter surfaces. Filter samples were subsequently analyzed for total sulfur content by RTP personnel using energy dispersive X-ray fluorescence techniques. Occasionally, extractions were prepared for independent analysis of soluble sulfate content by ion chromatography, also at RTP.

The second sampling system consisted of a cloud water collector in which cloud droplets, accelerated through an inlet of suitable aerodynamic design, were impacted on a sintered glass rod where they coalesced and dripped into a glass container. Cloud water samples were analyzed on site for pH and mailed to RTP for ion chromatographic analysis of soluble sulfate.

$HC+NO_x+SO_2$ SYSTEMS

The auto exhaust experiments showed that the use of leaded fuels produced greater quantities of particulates, both in number and volume, and consequently, greater reductions in visibility than the use of unleaded fuels. The primary particulates of auto exhaust did not measurably influence the oxidation of SO_2. The measured loss of gaseous SO_2 in these experiments was not sufficient to account for the measured rate of production of aerosol volume. A substantial fraction of aerosol growth, therefore, appeared to be due to species other than sulfates.

Nevertheless, the volumetric production of aerosol provided the only measure of sulfate formation available prior to incorporation of the new sampling techniques described above. The data can be correctly interpreted as upper limits of sulfate production during those early experiments and showed that the average rate of SO_2 oxidation over the approximate 10 hour duration of each auto exhaust experiment (HC/NO_x ~6.1) was $\lesssim$1% $hour^{-1}$. Using upgraded sampling and analysis procedures in later experiments, with HC/NO_x ~50/1 and substantially better time resolution in data collection, enhanced rates of SO_2 oxidation of ~5% $hour^{-1}$ were observed during the first two hours of irradiation. Subsequently, little or no SO_2 oxidation or volumetric aerosol growth was observed through the remainder of each experiment (up to four additional hours).

HAZE AND FOG + SO_2 SYSTEMS

This initial laboratory investigation of the importance of catalytic oxidation of SO_2 in typical wet industrial haze and urban fog demonstrated the importance of the phenomenon on local conditions and suggests potential significance on a broad, synoptic scale. Of equal importance, methods for detailed investigation of the phenomenon were developed. Specific results may be summarized as follows:

1. No discernible catalytic oxidation of SO_2 was observed in haze with b_{scat} of about $2.3 \times 10^{-4} m^{-1}$ and catalyst concentrations (V, Mn or Fe) in solution droplets of 10^{-4}M or less. Whether or not this

result pertains to more dense haze (i.e., greater liquid water content) with the same catalyst concentrations was not investigated.

2. Substantially enhanced oxidation rates were observed in nonirradiated dense haze (b_{scat} from 23 to 11.5 x 10^{-4} m^{-1}) with Fe and Mn catalyst in solution concentrations of the order of 10^{-3}M. These concentrations are equivalent to ∿1 μg m^{-3}, which is typical of urban plumes, and resulted in sulfate concentrations of up to 80 μg m^{-3} in the air mass within 30 minutes. Average oxidation rates up to 5% $hour^{-1}$ were observed, but we suspect that the actual rate exceeded that value in the very early portion of the experiment and approached zero by the end of the 30 minute interval (see #5 below).

3. As a continuation of each dense haze experiment, fog was formed on the haze aerosol and maintained for an additional 25 minutes. Catalytic oxidation persisted during this period at approximately the same average rate to yield up to 360 μg ml^{-1} of sulfate in the liquid water, corresponding to ∿140 μg m^{-3} in the air mass. The measured concentrations of Mn and Fe in the fog water were each ∿2.5 μg ml^{-1}, corresponding to typical urban plume values of 1 μg m^{-3}. Typical pH of the liquid water was about 3.

4. The haze and fog experiments demonstrated a direct dependence of sulfate production on concentration of catalyst in the solution droplets and on liquid water content of the aerosol. The direct dependence of sulfate production on SO_2 concentration was demonstrated in fog experiments. While data are not available for haze experiments, a similar dependence probably exists. These data are not sufficient to allow a determination of reaction rates.

5. From measurements in successive fogs produced in the same air mass, it is apparent that all of the catalytic oxidation of SO_2 that does occur in the haze-fog water occurs prior to the end of the first 25 minute-long fog. It is suspected, therefore, that the actual rate of oxidation is more rapid than the observed average rate of

~5% per hour but that this rate did not persist even for 25 minutes. It is further suspected that the total production of sulfate is limited by the decrease of pH of the solution droplets which accompanies the increasing concentration of SO_4.

6. There appears to be no synergistic effect on the rate of SO_2 oxidation due to irradiation of fog or haze composed of catalytic solution droplets. The amount of sulfate produced in each experiment of this type was about equivalent to the sum of what would be expected from independent photooxidation and catalytic oxidation experiments in the same conditions.

This preliminary investigation of the role of the in-fog or in-cloud oxidation of SO_2 confirmed that the catalytic oxidation of SO_2 in the solution droplets of clouds, fogs, and hazes may contribute significantly to the total oxidation of SO_2 in the atmosphere. The observed dependence of the catalytic oxidation of SO_2 on SO_2 concentration and type as well as concentration of catalysts demonstrated that this mechanism may be responsible for the major amount of SO_2 oxidation observed in urban plumes and especially in the plumes of specific heavy industries. In such plumes, typical conditions of high SO_2 and abundant potential catalysts as well as high LWC creat ideal conditions for the catalytic oxidation of SO_2. In remote areas where low levels of SO_2 and potential catalytic materials are common, the photooxidation of SO_2 may be the dominant mechanism for the conversion of SO_2 to sulfate.

SECTION 3
RECOMMENDATIONS

Discrepancies between the rate of SO_2 oxidation as determined by XRF analysis of the sulfur content of aerosol samples and the SO_2 oxidation rate calculated from EAA aerosol size distribution data indicate the need for direct determinations of aerosol composition in future auto exhaust experiments. This need is apparently the result of a mixed aerosol composition. It is also recommended that future experiments be performed using short time resolution (i.e., ~15 min) to investigate the influence of HC/NO_x ratio on the rate of production of sulfate and aerosol as a function of time after SO_2 introduction into the system. These experiments should be designed to reveal the proportion of the total aerosol produced which is attributable to sulfate, and if possible, to investigate the nature of the nonsulfate compounds contributing to aerosol growth. Pertinent related measurements should be made to help elucidate information on the effect of the ozone peak on photooxidation of SO_2.

This initial set of wet haze and fog experiments was heavily involved with development of experimental techniques, and with attempting to determine which experimental parameters were important by scanning catalytic oxidation processes under widely different conditions. It is now necessary to examine the functional relationships of sulfate production and the variables that were demonstrated to be important on this program. It is recommended that additional experimentation be conducted to generate these functional relationships.

As with all smog chamber experiments, initial effort must be devoted to the demonstration of repeatability of results. Based on current results, it is very important in the future to use the shortest available time resolution in acquisition of data so that temporal variations in the rate

of catalytic oxidation of SO_2 in wet aerosols can be determined. The greatest potential for achieving high temporal resolution appears to rest with the use of the fog water collector which could be modified to provide independent 1 ml samples at approximately one minute intervals in dense fog (b_{scat} >460 x $10^{-4}m^{-1}$) and perhaps 5 minute intervals in light fog (e.g., b_{scat} ~100 x $10^{-4}m^{-1}$). Under dense haze conditions (b_{scat} ~23 x $10^{-4}m^{-1}$), it appears appropriate to reduce sampling time of the heated air inlet system by a factor of at least three, providing temporal resolution of approximately 5 minutes.

Future experiments should be designed to separate some of the variables that appear, from current results, to be important. In the broadest sense, by the simple expedient of introducing SO_2 into the system after the pre-fog haze has come to equilibrium but before expansion to produce fog, a much better definition of oxidation rates in fog could be obtained, expecially with the recommended improved temporal resolution.

Some of the data to date indicating the importance of catalyst concentration in solution droplets also illustrate the joint effect of two different catalysts, which probably are synergistically more effective than either alone. Careful consideration should be given in the future to isolating potentially catalytic materials as well as investigating synergistic effects of mixed materials.

The existing haze data correspond to conditions in clean urban air and contaminated urban plumes. To investigate these specifics, both liquid water content and catalyst concentration in solution droplets were altered simultaneously. Future experiments investigating these variables independently and at intermediate ranges are desirable. Again, improved temporal resolution is required to determine the importance of duration of haze on total sulfate production.

With the quantitative importance of individual variables established, improved numerical modeling can be expected. Further chamber experiments in which real world industrial and urban plumes are simulated will be important for verification of modeling results.

SECTION 4
EXPERIMENTAL FACILITIES

The Calspan smog chamber has been described in substantial detail elsewhere (e.g., Kocmond et. al., 1973) and will only briefly be reviewed here. The facility itself consists of a cylindrical chamber 9.14 meters (30 feet) in diameter and 9.14 meters (30 feet) high enclosing a volume of 590 m^3 (20,800 ft^3). A cut-away view of the entire facility is illustrated in Figure 1. The 1.25 cm thick steel wall of the chamber is designed to withstand pressure differentials of 60 kilopascals (6.1 m of water); however, the Pyrex cover plates of the irradiation system currently limit pressure differentials to about 3.9 kilopascals (40 cm of water). The inner chamber surface is coated with a fluoroepoxy-type urethane (developed at the Naval Research Laboratory, Washington, D.C.) which has surface energy and reactivity properties comparable to those of FEP Teflon. Illumination within the chamber is provided by 28.6 kw of fluorescent blacklight and sun lamps installed inside 24 lighting modules and arranged in eight vertical channels attached to the wall of the chamber. Each lighting module contains two 40-watt sun lamps, eight 85-watt high output black lamps, and two 215-watt specially-produced black lamps. The lighting modules are covered with 0.5 cm thick Pyrex glass and are air cooled and sealed from the chamber working volume in order to minimize sources of contamination inside the chamber. Measured light intensity using the k_d $[NO_2]$ method reported by Stedman & Niki (1973) is $k_d \sim 0.35$ min^{-1}. A variety of light intensities can be provided by selectively turning off some of the light modules and lamps. A photograph of the interior of the chamber with the lighting system turned on is shown in Figure 2.

Air purification for the chamber is accomplished by recirculating the air through a series of absolute and activated carbon filters. Nearly all gaseous contaminants and particulate matter can be removed from the chamber air in

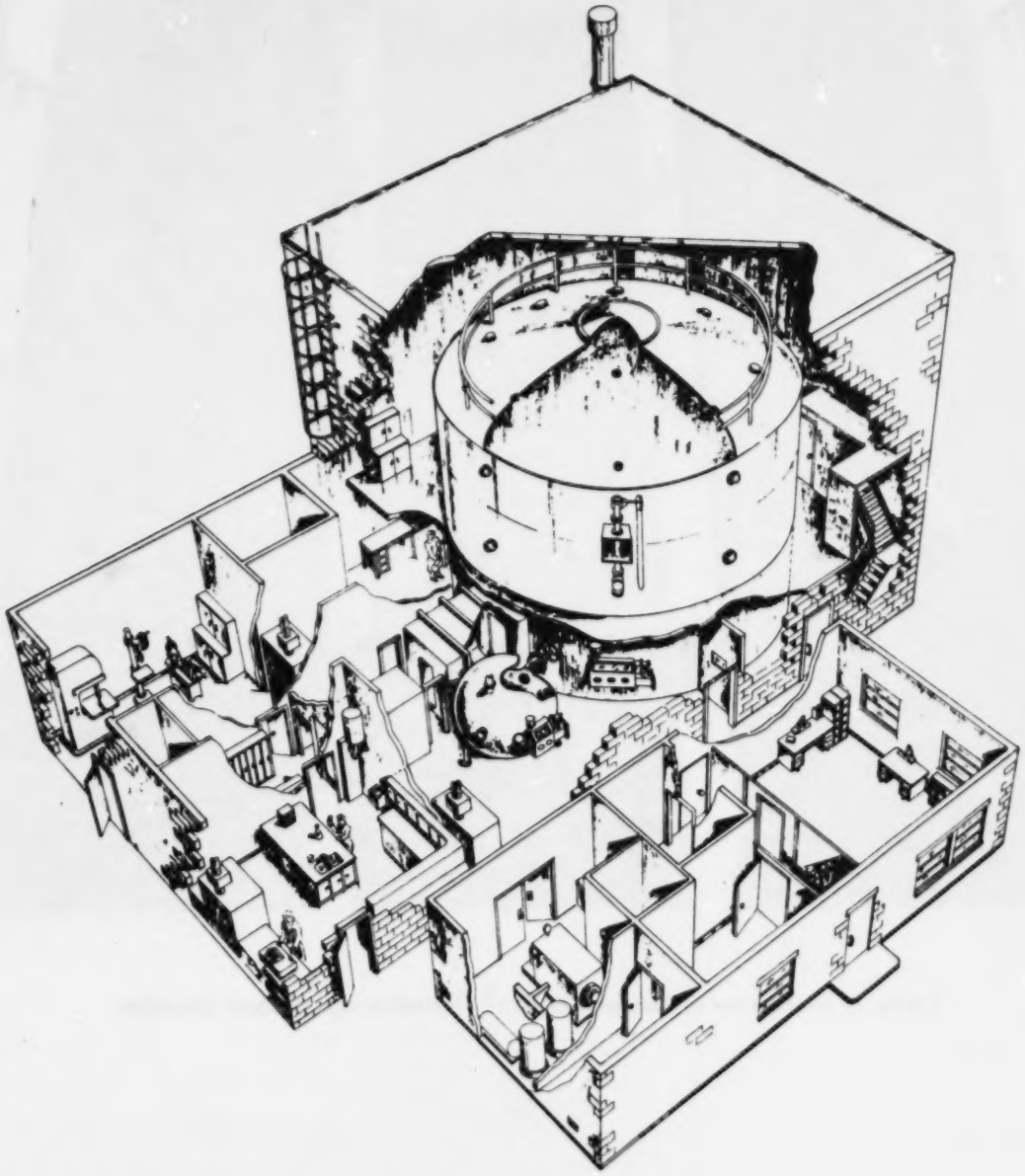

Figure 1. Cut-away view of Calspan Environmental Simulation Facility.

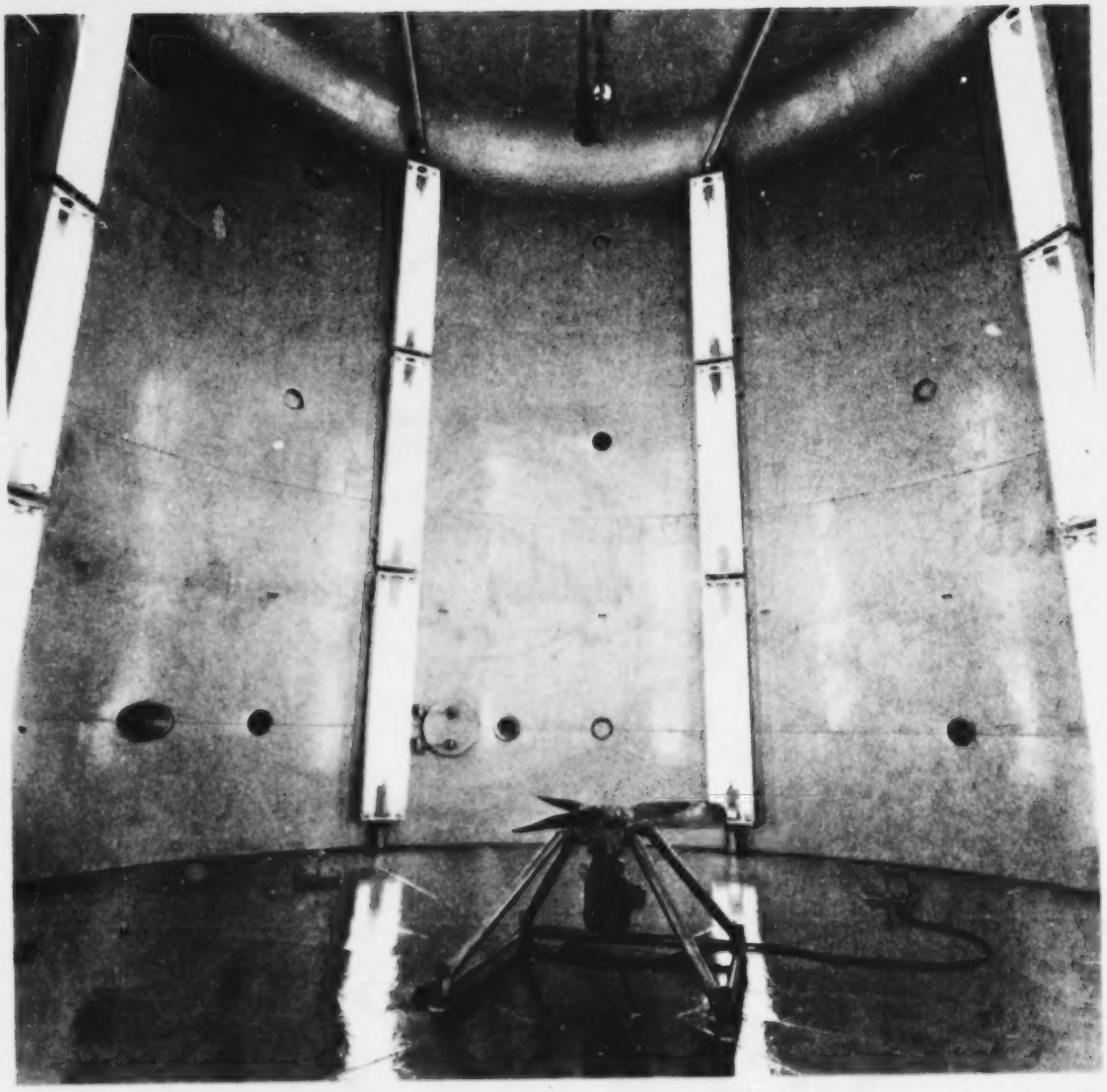

Figure 2. Inside view of Calspan's 600 m^3 Photochemical Aerosol Chamber.

about four to five hours of filtration. Filtered air generally contains no measurable Aitken particles, less than 0.1 ppm NO_x, 0.2 ppmC non-methane HC, and no measurable SO_2 or ozone.

Chamber washdown, humidification, and dehumidification systems were in frequent use during this program's tests. The recirculating washdown system consists of a stainless steel spray head which rotates on two axes and can wet all of the chamber surfaces with distilled water or cleaning solution. Generally, the procedure is to first wash the chamber surfaces with a 5% solution of a laboratory glass cleaning agent followed by two or three rinsings with tap water and two final rinsings with distilled water. Drying is accomplished by fresh air flushing followed by air filtration. The washdown system is also used to wet the chamber wall prior to a cloud forming experiment. Chamber humidity is increased by spraying distilled water into the chamber from a remotely-operated spray nozzle near the chamber top. Nuclei which are introduced by the evaporating spray droplets are removed by absolute particle filters during the air filtration cycle. Chamber dehumidification, when needed, is accomplished by passing the chamber air over refrigeration coils to remove excess water. The system, designed and fabricated at Calspan, is capable of controlling humidity down to about 20% RH.

Instrumentation used to monitor aerosol behavior and reactant concentrations within the chamber includes a Bendix Model 8002 chemiluminescent ozone analyzer, Model 8101-B nitrogen oxides analyzer, Model 8300 total sulfur analyzer, and the Model 8201 reactive hydrocarbon analyzer, a Hewlett-Packard 5750 gas chromatograph, a Thermo Systems Model 3030 Electrical Aerosol Analyzer (EAA), an MRI Integrating Nephelometer, a Gardner Associates small particle detector, a GE condensation nucleus counter, a Royco Model 220 Optical Particle Counter, and one of Calspan's static diffusion chambers (used to measure cloud condensation nuclei concentrations). A Meloy flame photometric total sulfur analyzer on loan from the EPA was also used for these experiments. A Royco Model 225 Optical Particle Counter was available during the last half of the current program. An isokinetic sampling inlet was designed and employed for particle sampling of chamber aerosols with minimal losses.

During the first half of this project, aerosol collection for determinations of sulfate (and occasionally nitrate and ammonium) contents was provided by filtering selected amounts of chamber air through Pallflex 2500 QAO Tissuquartz filters. A Millipore filter system (142 mm) and a Gelman hi-vol sampler (105 mm) were used for the sample collection. As a result of inconsistencies in the measured concentration of sulfate from samples collected in this manner, an alternative system was designed to reduce the possibility of artifact sulfate formation. The new system was designed around a temperature-controlled heated sampling inlet. For a detailed discussion of this sampling system, refer to Section 5 entitled Aerosol Sampling and Sulfate Analysis.

During in-fog experiments, bulk samples of fog water suitable for chemical analysis were collected with Calspan's Fog Water Collector. This device as well as several other unique fog characterization instruments and techniques were developed at Calspan under various internal research programs to provide means for the accurate measurements of the microphysical characteristics of fogs. The use of the Fog Water Collector during the current program is discussed in Section 7.

SECTION 5
AEROSOL SAMPLING AND SULFATE ANALYSIS

Early in the project, the inconsistency of aerosol sulfate data indicated that representative determinations of the sulfate content of the aerosols were not being obtained. These inconsistencies were especially obvious in the preliminary in-cloud experiments in which relatively large quantities of sulfates were observed in background experiments where little if any sulfate should have been found.

Aerosol collections were initially made using a 142mm Millipore in-line filter holder. Aerosol samples on Tissuquartz filters were taken over a 30-minute period encompassing sample volumes of approximately 3.2 m^3. Subsequently, a Gelman hi-vol sampler was also used. With the hi-vol system, sample volumes of approximately 10 m^3 were passed through the filter over a 30-minute period. The barium perchlorate titration method (Fielder and Morgan, 1960) was used for sulfate analysis.

Numerous experiments were performed to test aerosol collection methods and microanalytical procedures. These culminated in the demonstration that filtered SO_2 injected into particle free air and drawn through Tissuquartz filters moistened with doubly distilled water was oxidized sufficiently to produce serious error in the experiments that we were attempting. These experiments precipitated an internal research and development project at Calspan which resulted in what we believe to be an acceptable aerosol sampling technique. In addition, the wet chemical technique for sulfate analysis was replaced by energy dispersive X-ray fluorescence analysis of filter samples and frequent analysis of filter extractions by ion chromatography. Both of these latter efforts were provided by the EPA at Research Triangle Park, North Carolina and are gratefully acknowledged. Since XRF analysis provides a measure of total elemental sulfur present on the sample, careful attention

was required to minimize sorption of SO_2 and artifact sulfate formation on the filter surfaces. Previous investigations by Piersen et. al.,(1976) and Byers and Davis (1970) had shown that teflon membrane filters satisfied these requirements. Thus 37mm diameter fluoropore membrane filters (0.5 μm pore diameter) which could be analyzed directly in the XRF device were chosen for use on the program. Use of these filters also provided samples of sufficient quantity to permit extraction and independent analysis of soluble sulfate content by ion chromatography for occasional verification of the interpretation of the elemental sulfur measurement as sulfate.

Additional precautions were required to minimize catalytic oxidation of SO_2 on the filters during sampling of in-cloud or haze experiments. At the relative humidities of >90% required in the experiments, it was anticipated that significant amounts of liquid water could potentially collect on the filter. Two choices were considered to reduce the potential for the catalytic oxidation of SO_2 on the filter surfaces during sample collection: (1) remove the SO_2 from the sample prior to its exposure to the filter; or (2) prevent liquid water from accumulating on the filter.

The feasibility of applying an SO_2 denuder such as the one described by Durham, Wilson, and Bailey (1976) was studied. The denuder selectively removes SO_2 by diffusion to the walls of a tube coated with lead dioxide. The residence time of the sample in the tube is chosen such that only a minimal amount of the aerosols (which have much smaller diffusion coefficients than gaseous SO_2) is lost to the walls while the major portion of the SO_2 is scavenged. Because of flow rate requirements of the sampling system, no acceptable denuders system could be devised.

The alternative would be to devise a method for elimination of the collection of liquid water. In a typical worse case experimental condition, chamber air might be slightly supersaturated at perhaps 20°C. By heating this air to 70°C prior to filtration, the relative humidity would be reduced to 7% and no substantial quantities of liquid water would be collected. The 70°C temperature would not produce a discernible loss of sulfuric acid.

Following heat transfer calculations which showed that these conditions could be met in a laminar flow inlet of reasonable configuration, a heated sampling inlet was designed, constructed and installed in the chamber (Anderson et. al., 1977) under Calspan Internal Research and Development funding. A schematic diagram of the heated sampling inlet is presented in Figure 3.

The 30mm ID stainless steel tube through which the sample is drawn is located in the center of the vertical configuration in Figure 3. Concentric with the stainless steel sampling tube is a teflon sleeve with 1/4" thick walls. This sleeve serves two purposes; first, it acts as an insulator to prevent significant heat losses into the chamber; and, secondly, it serves as an inert outer material which will not contribute to the catalytic or photochemical reactions under investigation. Heating tape is located between these two concentric tubes. Thermocouples are located at the heater and inside the sampling tube near the filter to monitor temperature. The temperature within the tube is controlled by an automatic temperature control circuit which is capable of holding the tube temperature to within $\pm$ 1°C following an initial warm-up period.

For the latter stages of the program involving in-cloud (in-fog) experiments, samples of cloud water ($\sim$10 ml) were obtained with Calspan's Fog Water Collector.* Samples of fog water were collected in addition to filter samples. The liquid water samples were analyzed by ion chromatography and provided some of the most significant data from the in-cloud experiments (see Section 7).

*The Fog Water Collector draws air through four narrow vertical openings located symmetrically about a vertical glass column. The sample velocity corresponding to a flow rate of about 1.9 m^3/min is sufficient to result in impaction upon the glass column of most of the fog droplets greater than one micron diameter. The fog water then drips from the glass column into a glass sample bottle.

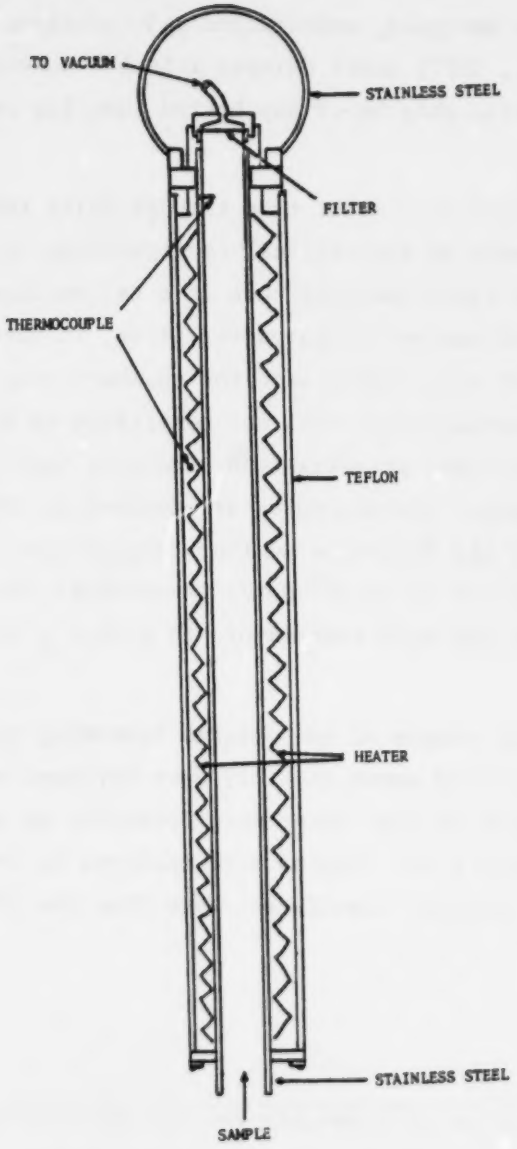

Figure 3. Schematic Drawing of Heated Sampling Inlet

SECTION 6

SO_2 PHOTOOXIDATION IN HC + NO_x + SO_2 SYSTEMS

The first series of tests performed under this contract were devoted to studies of the photooxidation of SO_2. Of particular interest were the possible influences of specific hydrocarbons as well as particulates to the rate of SO_2 photooxidation. A complete log of the 65 tests performed as part of this group of experiments is given in Table 1. As has been our practice in the past, many experiments involved clean air + SO_2 irradiations to establish chamber reactivity and to assure the absence of memory effects of preceding experiments on H_2SO_4 formation.

THE HC + NO_x + SO_2 SYSTEM

During an earlier program, a number of smog chamber experiments were performed at Calspan using various combinations of hydrocarbon systems. The most frequently employed test mixtures (propylene + NO_x systems with and without added SO_2) were selected on the basis that such reaction systems have been extensively modeled and comparisons of model predictions with chamber results would be possible. It was found from these previous experiments (Kocmond and Yang, 1975) that apparent synergistic effects in aerosol production and growth occur with the addition of SO_2 to the propylene + NO_x system. The maximum aerosol volumetric growth rate $[dv/dt]_{max}$ has always been found to be greater for the mixed system than the sum of the rates for propylene + NO_x and SO_2 alone. In the late stages of the experiment, after NO has been completely oxidized, abundant aerosol was formed but it has not been determined explicitly what fraction of the aerosol was actually sulfate. An additional series of tests was performed during the current phase program using the propylene + NO_x system with added SO_2. The cyclohexene + NO_x + SO_2 system is also very reactive in terms of aerosol production and was also tested.

TABLE 1
COMPLETE LOG OF CALSPAN SMOG CHAMBER EXPERIMENTS

RUN NO.	DATE	SYSTEM	SO_2 (ppm)	COMMENTS
A	11/10/75	LIGHT INTENSITY	CHECK	$k_d[NO_2]$ 0.41 min^{-1} NEW LAMPS
1	11/18/75	SO_2 + CLEAN AIR	0.15	EXPERIMENTS 1-4; BACKGROUND REACTIVITY TESTS
2	12/8/75	SO_2 + CLEAN AIR	0.38	
3	12/8/75	SO_2 + CLEAN AIR	0.31	
4	12/10/75	SO_2 + CLEAN AIR	0.28	
5	12/10/75	SO_2 + 60 ppm CO	0.19	TEST OF OH SCAVENGING
6	12/12/75	$C_3H_6 + NO_x$	0	EXPERIMENTS 6-13: TEST OF HC EFFECTS ON R_{SO_2}
7	12/15/75	$C_3H_6 + NO_x$	0	
8	12/16/75	$C_3H_6 + NO_x$	0	
9	12/18/75	$C_3H_6 + NO_x + SO_2$	0.31	
10	12/30/75	$C_3H_6 + NO_x + SO_2$	0.28	
11	1/8/76	CYCLOHEXENE + NO_x + SO_2	0.40	
12	1/12/76	CYCLOHEXENE + NO_x + SO_2	0.34	
13	1/13/76	CYCLO + PROP + NO_x + SO_2	0.40	
14	1/15/76	AUTO EXHAUST + NO_2 W/NUCLEI	0.50	EXPERIMENTS 14-19: AUTO EXHAUST IRRADIATION WITH AND WITHOUT COMBUSTION NUCLEI - LEADED VS. UNLEADED FUEL
15	1/16/76	AUTO EXHAUST W/NUCLEI	0.38	
16	1/20/76	AUTO EXHAUST W/O NUCLEI	0.50	
17	1/30/76	AUTO EXHAUST W/O NUCLEI	0.30	
18	2/3/76	AUTO EXHAUST DARK rx	0.44	
19	2/4/76	AUTO EXHAUST W/O NUCLEI	0.34	
20	2/5/76	SO_2 + CLEAN AIR	0.55	BACKGROUND REACTIVITY EXPERIMENTS
21	3/9/76	SO_2 + CLEAN AIR	0.65	
22	3/10/76	AUTO EXHAUST (Pb): DARK rx	0.78	EXPERIMENTS 22-26: AUTO EXHAUST IRRADIATION WITH AND WITHOUT COMBUSTION NUCLEI - LEADED FUEL
23	3/11/76	AUTO EXHAUST (Pb): W/NUCLEI	0.52	
24	3/16/76	AUTO EXHAUST (Pb): W/NUCLEI	0.62	
25	3/16/76	AUTO EXHAUST (Pb): W/O NUCLEI	0.44	
26	3/22/76	AUTO EXHAUST (Pb): W/O NUCLEI	0.40	
27	4/5/76	SO_2 + 1.1 ppm NO_x	0.50	TEST NO_x EFFECT ON R_{SO_2}
28	4/27/76	SO_2 + CLEAN AIR	0.38	BACKGROUND rx ABORT EXPERIMENTS 29-40 INVOLVE IN-CLOUD SO_2 ADDITIONS
29	5/3/76	SO_2 + CLOUD (DARK ONLY)	0	
30	5/4/76	SO_2 + CLOUD (DARK ONLY)	0.18	
31	5/4/76	SO_2 + CLOUD (DARK ONLY)	0.25	
32	5/4/76	SO_2 + CLOUD (DARK ONLY)	0.50	
33	5/6/76	SO_2 + CLOUD (DARK ONLY)	0.70	
34	5/6/76	SO_2 OVER WET FILTER	0.95	CHECK OF ON-FILTER OXIDATION
35	5/11/76	SO_2 + NaCl CLOUD	0.45	IRRADIATE 50 min
36	5/11/76	SO_2 + NaCl CLOUD	0.28	IRRADIATE 70 min
36a	5/13/76	LIGHT INTENSITY	CHECK	$k_d[NO_2] \sim 0.36$ min^{-1}

(continued)

TABLE 1 (continued)

RUN NO.	DATE	SYSTEM	SO_2 (ppm)	COMMENTS
37	5/16/76	CLOUD ONLY	0	BEGIN USING NEW FILTER FOR AEROSOL COLLECTION HIGH RH
38	5/18/76	SO_2 CLOUD	0.55	
39	5/18/76	SO_2 + CLEAN AIR	0.90	
40	5/18/76	SO_2 + CLOUD (DARK)	1.30	WET AIR BEFORE FILTER BACKGROUND rx CHECK EXPERIMENTS 41-60
40a	5/28/76	CLEAN AIR IRRADIATION	0	
41	5/28/76	SO_2 + CLEAN AIR	1.30	
42	6/9/76	SO_2 + CLEAN AIR	1.10	PERFORMED TO COMPARE AND DEVELOP SULFATE ANALYSIS PROCEDURES
43	6/9/76	SO_2 + CLEAN AIR	1.00	
44	6/10/76	SO_2 + CLEAN AIR	1.10	
45	6/10/76	SO_2 + CLEAN AIR	1.10	REPLACE CHARCOAL FILTERS
46	7/16/76	SO_2 + CLEAN AIR	1.00	
47	7/20/76	SO_2 + CLEAN AIR	0.90	BEGIN USING HI-VOL SAMPLER
48	7/23/76	SO_2 + CLEAN AIR	0.92	WASH SMOG CHAMBER
49	7/29/76	SO_2 + CLEAN AIR	1.18	
50	7/29/76	SO_2 + CLEAN AIR	0.96	
50a	7/29/76	0.4M H_2SO_4 + CLEAN AIR	$<$ 0.01	EXPERIMENTS 50-54; INTRODUCE H_2SO_4 OF $(NH_4)SO_4$ DROPLETS INTO CHAMBER USING COLLISION ATOMIZER AND THEN COLLECT AEROSOL SAMPLE TIZZUE QUARTZ
50b	7/29/76	0.4M H_2SO_4 + CLEAN AIR	$<$ 0.01	
51	8/17/76	0.4M H_2SO_4 + CLEAN AIR	$<$ 0.01	
52	8/17/76	0.4M H_2SO_4 + CLEAN AIR	$<$ 0.01	
53	8/18/76	0.4M $(NH_4)_2SO_4$ + CLEAN AIR	$<$ 0.01	
54	8/18/76	0.4M $(NH_4)_2SO_4$ + CLEAN AIR	$<$ 0.01	
55	8/18/76	SO_2 + CLEAN AIR	0.95	BACKGROUND REACTIVITY MEASUREMENTS
56	8/19/76	SO_2 + CLEAN AIR	1.04	
57	8/20/76	CLEAN AIR ONLY	0	
58	8/20/76	RURAL AIR ONLY	$<$ 0.01	
59	8/20/76	SO_2 + RURAL AIR	0.55	
60	8/25/76	SO_2 + RURAL AIR (DARK rx)	0.55	
X1	1/25/77	AUTO EXHAUST (Pb): W/NUCLEI	0 45	BEGIN USE OF MODIFIED SAMPLING AND ANALYSIS TECHNIQUES
X2	3/15/77	AUTO EXHAUST (Pb): W/NUCLEI	0.40	
X3	3/16/77	AUTO EXHAUST (Pb): W/O NUCLEI	0.35	
X4	10/18/77	AUTO EXHAUST (Pb): W/O NUCLEI	0.55	
X5	10/19/77	AUTO EXHAUST (Pb): W/O NUCLEI	0.40	

Chemical and aerosol data for these experiments are summarized in Tables 2 and 3. In Table 2, the run number, date, relative humidity, reactant concentration and times to ozone and NO_2 max are shown. Table 3 summarizes the maximum particle concentration for each system, the initial and maximum volumetric production rates of aerosol (i.e., $[dv/dt]_1$ and $[dv/dt]_{max}$) and the computed initial SO_2 photooxidation rate as determined from electrical aerosol analyzer (EAA) data.

As in the past, values of the volumetric growth of the aerosols as measured by the EAA are used to estimate the rate of SO_2 oxidation. The basis for the calculation is the assumption that all of the aerosol growth is the result of the formation of sulfuric acid and its subsequent absorption of water from the air. The governing equation is:

$$-\frac{d[SO_2]}{dt} = \frac{dv}{dt}\ (\rho)\ (P)\ \left(\frac{MW_1}{MW_2}\right) \qquad (1)$$

where ρ is the density of the sulfuric acid droplet, P is the weight fraction of H_2SO_4 in the droplet, MW_1 is the molecular weight of SO_2, and MW_2 is the molecular weight of H_2SO_4.

The data in Table 2 show that for average propylene concentrations of about 3.1 ppmC and NO_x concentrations of about 0.5 ppm, the time to ozone peak is about 270 minutes and the corresponding time to NO_2 max is about 140 minutes.

The summary of aerosol data in Table 3 shows that the initial rate of SO_2 oxidation $(R_{SO_2})_i$ in the propylene + NO_x + SO_2 system is about 0.9% hr^{-1} and that for the cyclohexene + NO_x + SO_2 system was only 0.4% hr^{-1}. Presumably, the rate of SO_2 oxidation is relatively slow initially because of the competition for OH by reactions with hydrocarbon and NO_x species. Estimates made by investigators at Battelle suggest that only 1-2% of the OH radicals produced during this period is consumed by the reaction with SO_2. Later, when abundant aerosol is formed, the rate of SO_2 oxidation also increases. If all of the aerosol produced during this period were aqueous

TABLE 2

SUMMARY OF CHEMISTRY DATA FROM HC + NO_x AND HC + NO_x + SO_2 IRRADIATIONS

RUN NO.	DATE	SYSTEM	RH	HC	NO_i	NO_{2_i}	$[O_3]$ max	TIME TO $[O_3]$ max	TIME TO $[NO_2]$ max
			%	ppmC	ppm	ppm	ppm	min	min
6	12/12/75	PROP + NO_x	25	2.9	.45	.035	.620	345	210
7	12/15/75	PROP + NO_x	35	3.2	.45	.09	.640	260	120
8	12/16/75	PROP + NO_x	45	3.0	.45	.06	.530	270	140
9	12/18/75	PROP + NO_x + SO_2	40	3.0	.45	.07	.420	240	140
10	12/30/75	PROP + NO_x + SO_2	45	3.1	.46	.12	.495	235	140
11	1/8/76	CYCLO + NO_x + SO_2	30	–	.44	.03	.385	310	180
12	1/12/76	CYCLO + NO_x + SO_2	30	3.2	.45	.04	.400	320	190
13	1/13/76	CYCLO + PROP + NO_x + SO_2	35	3.3	.47	.04	.535	330	180

TABLE 3

SUMMARY OF AEROSOL DATA FROM HC + NO_x & HC + NO_x + SO_2

RUN NO.	DATE	SYSTEM	Nmax	$\frac{dv}{dt}$ (i) *	$\frac{dv}{dt}$ (max) **	$R_{SO_2(i)}$ ***
			cm^{-3}	$\mu m^3 hr^{-1} cm^{-3}$	$\mu m^3 hr^{-1} cm^{-3}$	EAA $\% hr^{-1}$
6	12/12/75	PROP + NO_x	1.3×10^5	0.1	10.6	–
7	12/15/75	PROP + NO_x	9.0×10^4	0.1	10.2	–
8	12/16/75	PROP + NO_x	1.1×10^5	0.1	2.7	–
9	12/18/75	PROP + NO_x + SO_2	$>10^7$	16.5	206.1	0.8
10	12/30/75	PROP + NO_x + SO_2	9.0×10^6	16.1	201.8	0.9
11	1/8/76	CYCLO + NO_x + SO_2	7.0×10^5	9.2	680.0	0.4
12	1/12/76	CYCLO + NO_x + SO_2	2.0×10^5	8.4	720.0	0.4
13	1/13/76	CYCLO + NO_x + SO_2	3.5×10^5	8.2	570.0	0.4

* INITIAL AEROSOL VOLUME FORMATION RATE

** MAXIMUM AEROSOL VOLUME FORMATION RATE

*** INITIAL RATE OF SULFUR DIOXIDE OXIDATION CALCULATED FROM EAA DATA, USING EQUATION 1

sulfate, (note $[dv/dt]_{max}$ values in Table 3) equivalent SO_2 photooxidation rates of 30-50% hr^{-1} would be derived. Since no such loss of SO_2 was observed, it appears that most of the aerosol produced is nonsulfate in nature; however, the exact composition of the aerosol must still be determined. Consequently, R_{SO_2} values calculated from EAA data using Equation 1 represent upper bounds for the actual R_{SO_2} due to aerosol growth from components other than sulfuric acid. It is instructive to note that the initial aerosol volumetric production rate dv/dt is approximately two orders of magnitude lower in the HC + NO_x systems not containnng SO_2.

AUTO EXHAUST EXPERIMENTS

A number of auto exhaust irradiation experiments were performed in an effort to study and compare the rates of SO_2 photooxidation in the presence or absence of combustion nuclei. Both leaded and unleaded fuels were used in this series of tests. The experiments consisted of operating a 1972 Chevrolet with 350 CID engine at a cruise speed of 40 mph on a chassis dynamometer while a fixed portion of the auto exhaust was introduced into the chamber. Evaporative emissions were added to the system to supplement the HC content and to give initial conditions of 3.0 ppmC HC, 0.5 ppm NO_x and 0.5 ppm SO_2. Relative humidity was adjusted to 50%. For experiments directed toward studies of SO_2 oxidation in the absence of primary combustion nuclei, the air mixture following introduction of auto exhaust was first passed through the chamber absolute filter system. After achieving the desired initial conditions, with or without the presence of primary auto exhaust nuclei, the system was irradiated for periods of up to 11 hours.

Aerosol data from the auto exhaust irradiation experiments are summarized in Table 4. The table shows: the particle concentration at t = 0, i.e., time of lights on; the maximum particle concentration observed during irradiation, N (max); the t = 30 minutes and maximum aerosol volumetric production rates; the initial, maximum, and average SO_2 photooxidation rates as determined from electrical aerosol analyzer (EAA) data; and the average SO_2 photooxidation rates as determined from the aerosol sulfate analysis (XRF) data.

TABLE 4
LOG OF AUTO EXHAUST EXPERIMENTS*

EXPERIMENT	DATE	N (t = 0)	N (max)	$\frac{dv}{dt}$ (t = 30)	$\frac{dv}{dt}$(max)	$R_{SO_{2(i)}}$	$R_{SO_2\ (max)}$	$R_{SO_2\ (ave)}$	R_{SO_2}
		cm^{-3}	cm^{-3}	EAA $\mu m^3 hr^{-1} cm^{-3}$	EAA $\mu m^3 hr^{-1} cm^{-3}$	EAA $\%\ hr^{-1}$	EAA $\%\ hr^{-1}$	EAA $\%\ hr^{-1}$	XRF $\%\ hr^{-1}$
14 AE W/NUCLEI	1/15/76	3.7×10^4	5.0×10^5	13.8	30.8	0.4	0.9	0.7	–
15 AE W/NUCLEI	1/16/76	4.0×10^4	6.0×10^5	12.8	33.8	0.4	1.1	0.6	–
16 AE W/O NUCLEI	1/20/76	$< 10^3$	$> 10^7$	21.2	37.0	0.6	1.1	0.8	–
17 AE W/O NUCLEI	1/30/76	$< 10^3$	$> 10^7$	11.8	25.2	0.7	1.4	1.0	–
18 AE: Dark Rx	2/3/76	2.0×10^4	2.0×10^4	-1.0	2.7	< 0.1	< 0.1	< 0.1	–
19 AE W/O NUCLEI	2/4/76	$< 10^3$	$> 10^7$	3.8	26.6	0.2	1.3	0.9	–
22 AE (Pb): Dark Rx	3/10/76	1.0×10^5	1.0×10^5	1.2	2.4	< 0.1	< 0.1	< 0.1	–
23 AE (Pb) W/NUCLEI	3/11/76	1.1×10^5	2.0×10^6	9.0	58.0	0.3	1.9	0.9	–
24 AE (Pb) W/NUCLEI	3/15/76	1.5×10^6	5.0×10^6	18.8	73.0	0.6	2.3	1.3	–
25 AE (Pb) W/O NUCLEI	3/16/76	$< 10^3$	$> 10^7$	5.2	56.4	0.2	2.0	1.0	–
26 AE (Pb) W/O NUCLEI	3/22/76	$< 10^3$	$> 10^7$	7.0	46.4	0.3	2.0	1.0	–
X1 AE (Pb) W/NUCLEI**	1/25/77	–	–	–	–	–	–	–	0.8
X2 AE (Pb) W/NUCLEI**	3/15/77	2.0×10^5	2.0×10^6	1200	1200	34.6	34.6	11.0	4.3
X3 AE (Pb) W/O NUCLEI**	3/17/77	$< 10^3$	$> 10^7$	370	711	11.0	24.8	9.8	4.4
X4 AE (Pb) W/O NUCLEI***	10/18/77	$< 10^3$	$> 10^7$	–	–	–	–	–	2.2
X5 AE (Pb) W/O NUCLEI***	10/19/77	$< 10^3$	$> 10^7$	–	–	–	–	–	0.5

*HC - 2.0 ppmC (EVAPORATIVE EMISSION ADDED
**HC - 25 ppmC
***HC -> 50 ppmC

NO_x ~ 0.5 ppm
SO_2 ~ 0.5 ppm (0.3 to 0.6 ppm)
RH_i ~ 50%

Table 5 summarizes the time events of chemical and visibility changes during the course of the auto exhaust irradiation experiments. In this table are shown the duration of each experiment, the initial SO_2 and NO_x concentrations, time to NO_2 maximum, time to O_3 max (not reached in any of the experiments), and the initial and final b_{scat} values observed after 400 minutes of irradiation.

Using the modified aerosol sampling procedure with filter analysis by energy dispersive X-ray fluorescence (see Section 5), five additional auto exhaust + SO_2 irradiation experiments were subsequently performed and are included in Tables 4 and 5 as X1 through X5. These additional experiments were performed to determine the rate of SO_2 photooxidation before and after O_3 (max) is reached. In each of these experiments, large HC/NO_x ratios were obtained by introducing the exhaust emissions of an engine at fast idle under no load conditions. In two of the five experiments, additional HC was introduced from accidentally contaminated water used in chamber humidity control. Leaded fuel was used in all five tests.

During each test, filter samples were obtained at approximately 30-minute intervals. The quantity of data obtained as well as its consistent nature allow much more accurate interpretations of the experiments than the previous data analyzed by the aforementioned wet chemical technique. Two sets of plots have been generated from this more complete data: (1) measured concentration of sulfate in units of $\mu g/m^3$ versus time after the initiation of irradiation shown in Figure 4; and (2) calculated rate of SO_2 oxidation in units of %/hour versus time after the initiation of irradiation displayed in Figures 5 through 7.

After about two hours each of the experiments with the exception of X3 exhibit a decay in the rate of SO_2 oxidation to extremely low values, in some cases zero. In one experiment, the complete lack of oxidation was tracked for four hours using independent sample collections and analyses.

Referring only to experiments X1 and X2, the reduced rate of SO_2 oxidation appears to be correlated with the O_3 (max). Experiments X4 and X5 with larger HC/NO_x ratios which did not allow the appearance of O_3 (max) during the

TABLE 5
AUTO EXHAUST EXPERIMENTS - CHEMISTRY DATA

EXPERIMENT	DATE	LENGTH	SO_2	NO_x	tNO_2 (max)	tO_3 (max)	$b_{scat_{t=0}}$	$b_{scat_{t=400}}$
		min	ppm	ppm	min	min	$10^{-4}m^{-1}$	$10^{-4}m^{-1}$
14 AE W/NUCLEI	1/15/76	330	.50	.50	330	>330	0.34	1.19
15 AE W/NUCLEI	1/16/76	420	.38	.47	370	>420	0.41	1.19
16 AE W/O NUCLEI	1/26/76	690	.50	.50	420	>690	0.24	0.82
17 AE W/O NUCLEI	1/30/76	510	.30	.45	500	>510	0.24	0.72
18 AE:DARK Rx	2/3/76	180	.44	.55	---	---	0.72	0.64
19 AE W/O NUCLEI	2/4/76	586	.34	.44	570	>580	0.24	0.72
22 AE (Pb): DARK Rx	3/10/76	240	.78	.69	---	---	0.52	0.48
23 AE (Pb) W/NUCLEI	3/11/76	420	.52	.50	330	>420	0.48	2.60
24 AE (Pb) W/NUCLEI	3/15/76	400	.62	.51	350	>400	0.41	3.57
25 AE (Pb) W/O NUCLEI	3/16/76	420	.44	.40	400	>420	0.24	1.43
26 AE (Pb) W/O NUCLEI	3/22/76	400	.40	.53	350	>400	0.24	2.39
X1 AE (Pb) W/NUCLEI	1/25/77	400	.10	.45	30	100	---	---
X2 AE (Pb) W/NUCLEI	3/15/77	180	.15	.40	30	90	0.64	> 40
X3 AE (Pb) W/O NUCLEI	3/17/77	150	.25	.35	30	90	0.57	25.58
X4 AE (Pb) W/O NUCLEI	10/18/77	215	.30	.55	---	---	0.29	35.42
X5 AE (Pb) W/O NUCLEI	10/19/77	250	.70	.40	---	---	0.29	4.61

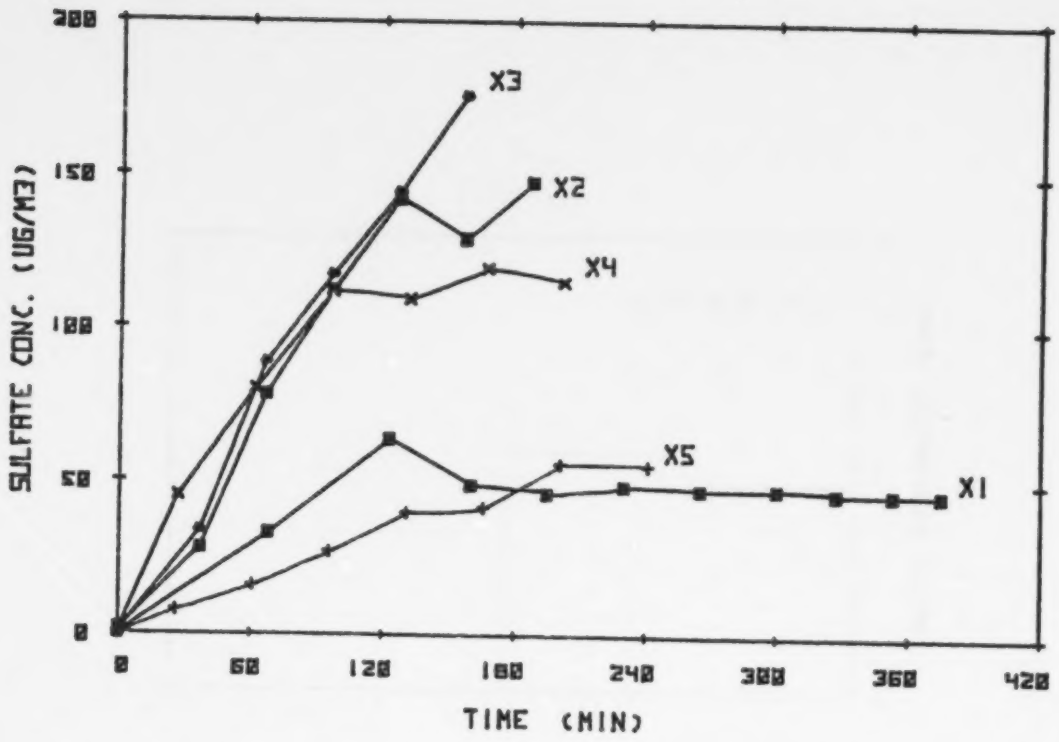

Figure 4. Sulfate Concentrations Versus Time for the Indicated Irradiated Auto Exhaust + SO_2 Experiments.

experiment, reveal the same decay in the rate of SO_2 oxidation after about the first two hours. Due to the redirection of the program towards in-cloud conditions, no effort was made to determine the behavior of the rate of SO_2 oxidation in systems containing a low HC/NO_x ratio.

The plots of R_{SO_2} shown in Figures 5, 6, and 7 indicate that there is no discernible difference in terms of the rate of SO_2 photooxidation between the systems containing the primary aerosol of the auto exhaust and the systems from which this primary aerosol has been removed. These findings corroborate the results of the previous set of experiments based only on EAA data and are exhibited in Table 4. In addition, the resolution resulting from obtaining filter samples so frequently allows us to observe that an apparent enhanced

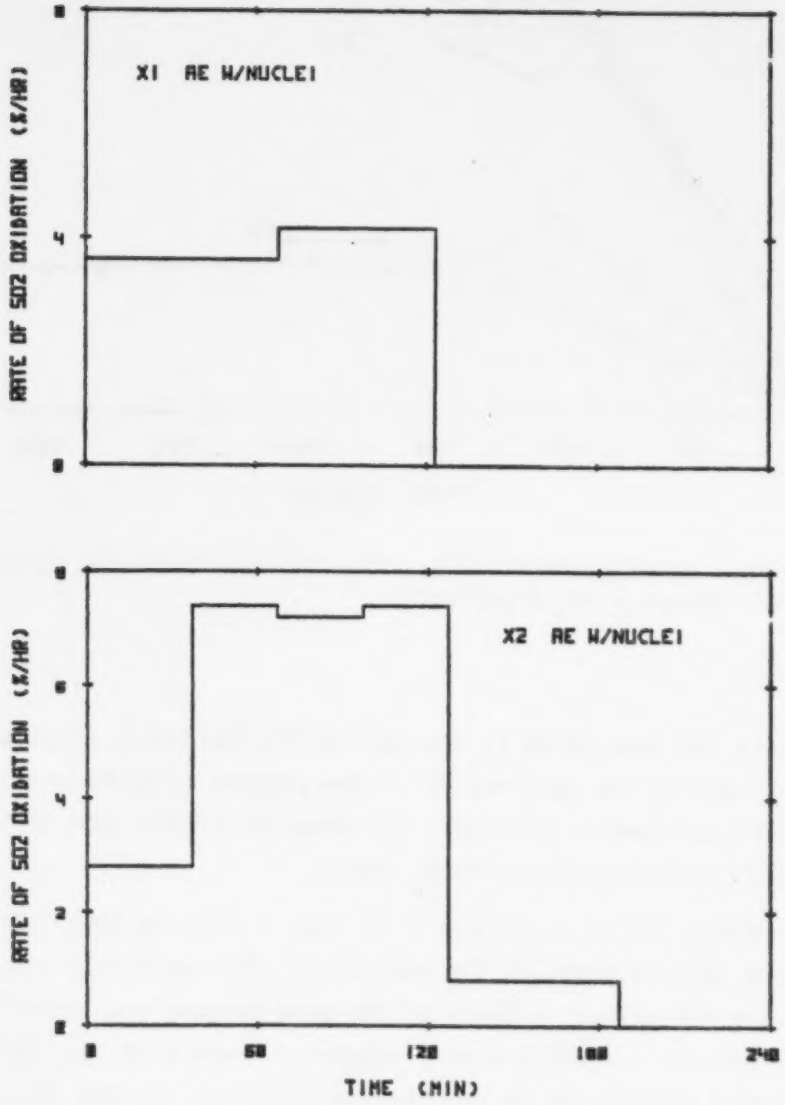

Figure 5. Rate of SO_2 Oxidation Versus Time for Indicated Irradiated Auto Exhaust + SO_2 Experiments

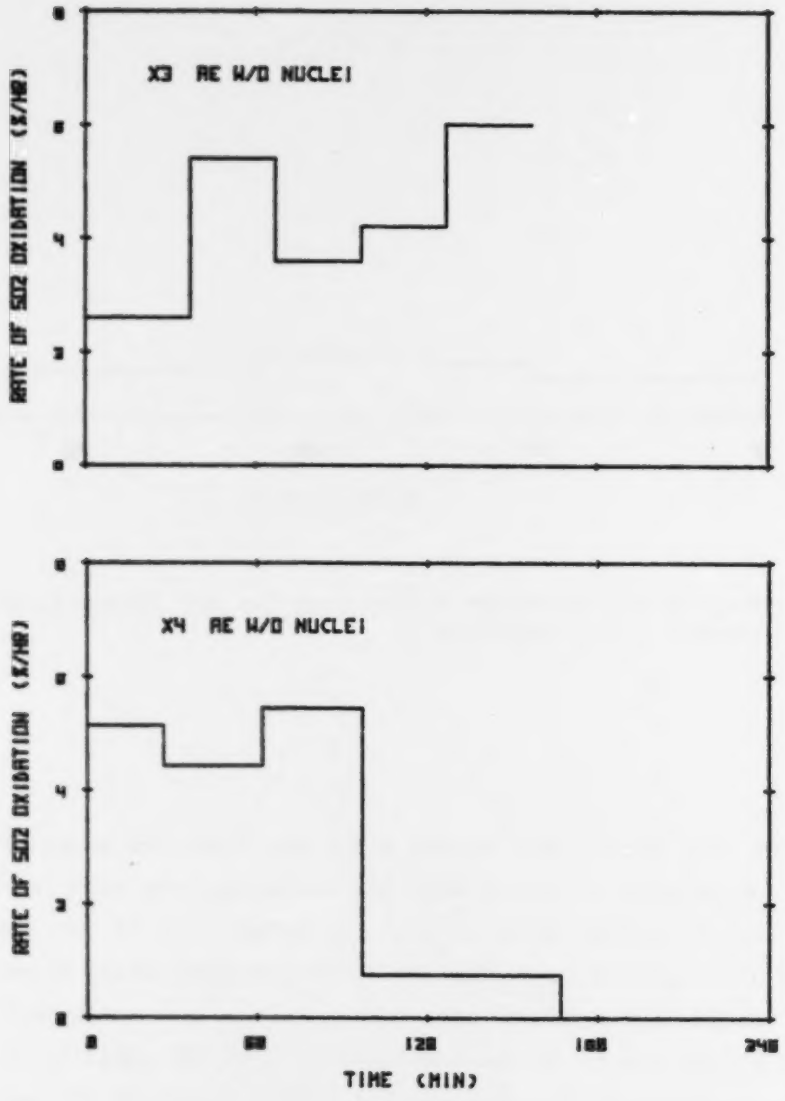

Figure 6. Rate of SO_2 Oxidation Versus Time for the Indicated Irradiated Auto Exhaust + SO_2 Experiments

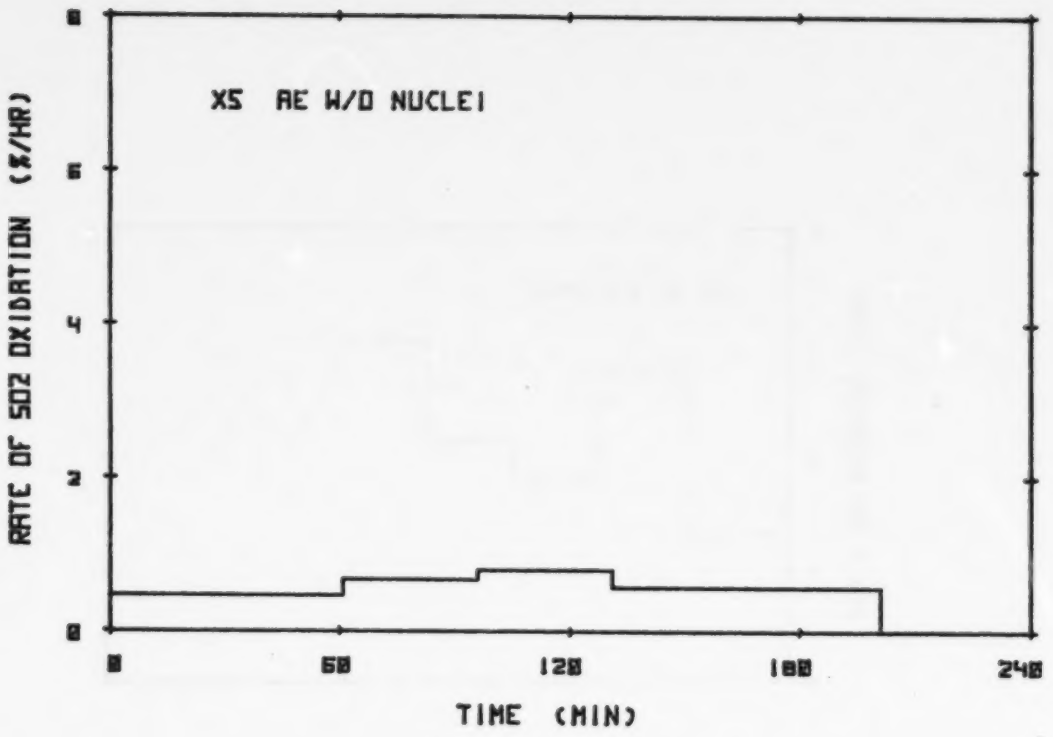

Figure 7. Rate of SO_2 Oxidation Versus Time For The Indicated Irradiated Auto Exhaust + SO_2 Experiments.

SO_2 oxidation rate occurs only during about the first two hours of the experiments. Following this period of high SO_2 oxidation, the rate as well as volumetric aerosol growth falls to very low values. It is not known if these results are also applicable to the earlier experiments using a lower HC/NO_x ratio. It should be recognized that five tests are not sufficient to make unqualified judgements as to the mechanism or even the qualitative form of the rate of SO_2 oxidation in the auto exhaust + SO_2 irradiated system. As a result, these findings should be considered tentative.

From the data summaries in the tables, as well as the tentative results shown in Figures 5, 6 and 7, the following points can be made concerning irradiated HC + NO_x + SO_2 systems.

1. Initial particle number concentrations were an order of magnitude higher for the auto exhaust tests in which leaded fuel was used. After lights were turned on, the maximum particle concentration and the rates of production of additional aerosol were also higher by a factor of about 2 for the leaded fuel cases. Maximum production of new particles was greater in experiments in which primary particulates were removed, confirming that significant amounts of volumetric growth occurs on existing primary aerosols.

2. For the first series of auto exhaust experiments, the average photooxidation rate of SO_2 as determined from measured volumetric aerosol growth was about the same ($\sim$1% hr^{-1}) with or without nuclei. In these tests, the HC/NO_x ratio was about 6:1 and the reactivity of the HC was not sufficiently high to allow complete oxidation of NO in less than about six hours. (By contrast NO dissappearance normally occurred in slightly more than two hours when propylene or or cyclohexene were used under equivalent conditions). In similar auto exhaust tests containing HC/NO_x ratios greater than 50:1, an apparent enhanced rate of photooxidation of SO_2 ($\sim$5% hr^{-1}) was observed during the first two hours of the experiments from XRF analysis of filter samples. Following this period of apparent enhanced SO_2 oxidation there was little if any further oxidation of SO_2 or volumetric aerosol growth. This behavior appears to be independent of the presence of the primary aerosol or the occurrence of O_3 (max). It is not known if the systems containing HC/NO_x ratios of 6:1 display the same behavior of SO_2 photooxidation.

3. In available data, the photooxidation rates for SO_2 as determined by XRF analysis of filter samples were less than the SO_2 oxidation rates determined from EAA data. This discrepancy suggests that the aerosol composition in the experiments was of a mixed nature (i.e., organics, nitrates, plus sulfates), assuming the EAA data is reliable.

4. The largest b_{scat} values (at t = 400 min) were observed for the leaded fuel experiments.

5. No appreciable dark reaction was observed for either the leaded or unleaded auto exhaust cases; i.e., no new aerosol was formed in the dark prior to irradiation.

SECTION 7

CATALYTIC SO_2 OXIDATION IN CLOUDS, FOGS AND HAZES

The measured rates of SO_2 photooxidation of a few tenths of a percent per hour (Gerhard and Johnstone, 1955; and Kocmond et. al., 1975) are not sufficient to explain the approximate four day lifetime of SO_2 in the atmosphere (Junge, 1960). In order to produce an atmospheric lifetime of four days, the actual rate of SO_2 oxidation must be almost an order of magnitude greater than that apparently due to photooxidation. One likely mechanism responsible for higher rates of atmospheric SO_2 oxidation is the catalytic oxidation of SO_2 in cloud, fog, or haze droplets containing high concentrations of heavy metals ($>10^{-4}$M).

Noted investigations of the catalytic oxidation of SO_2 in aqueous solutions containing heavy metals have been performed by Junge and Ryan (1958) and Johnstone and Coughanowr (1958). While the experimental techniques used by the former group have questionable pertinence to actual conditions occurring in the atmosphere, qualitatively, the results are of interest. They found the rate of catalytic oxidation of SO_2 in an aqueous solution to be dependent upon the SO_2 concentration, pH of the solution, and the type and concentration of heavy metal catalyst. Suspending 300 μm diameter droplets from a glass fiber, Johnstone and Coughanowr (1958) observed rates of SO_2 oxidation within the droplets corresponding to about 60% hr^{-1} when extrapolated to liquid water contents of 0.2 g/m^3 and ambient SO_2 concentrations of 1 ppm. In a more recent investigation, Barrie and Georgii (1976) essentially repeated the work of Johnstone et. al., (1958) using refined techniques and SO_2 concentrations more likely to be found in clouds. The results of the Barrie and Georgii (1976) investigation were extrapolated to clouds containing 0.1 g/m^3 of liquid water, heavy metals Mn^{+2} and Fe^{+2} at concentrations of 10^{-5}M each, and 20 ppb of

ambient SO_2. Their estimated in-cloud oxidation rate of SO_2 varied from 0.08 to 2.2% hr^{-1}. They found the rate of SO_2 oxidation to be dependent upon temperature, SO_2 concentration, pH, and type as well as concentration of catalyst.

Junge and Ryan (1958) also proposed that the presence of NH_3 in the solution droplets containing heavy metal ions might produce a more active system in terms of SO_2 oxidation. The "catalytic" oxidation of SO_2 in aqueous systems by NH_3 has since been expounded by Scott and Hobbs (1967), McKay (1971), Miller and DePena (1972), and Easter and Hobbs (1974). However, recent reviews of the proposed mechanism (Barrie et. al., 1974; and Beilke, et. al., 1975) suggest that it will not contribute significantly to SO_2 oxidation in the atmosphere for values of pH normally observed in cloud droplets (typically between 4 and 5). Barrie et. al.,(1974) conclude that the major function of the SO_2-NH_3-liquid water system is not the conversion of SO_2 to sulfate but rather the conversion of sulfuric acid aerosol and ammonia gas to ammonium sulfate.

At Calspan, unique chamber facilities allow the repeatable generation of fogs, clouds, or hazes which have characteristics similar to those of the respective phenomena occuring in nature. As a result of the ability to accurately simulate and measure the microphysical features of these natural phenomena, we can determine, without the need for questionable extrapolations, the rate of SO_2 oxidation for typical cloud and haze conditions, and because of the large size of the chamber (590 m^3), with minimum wall effects.

Calspan performed two separate series of chamber experiments to investigate the role of the catalytic oxidation of SO_2 in the atmosphere. In the first series of experiments, hazes were produced in the chamber and SO_2 oxidation was monitored as concentrations of SO_2 and heavy metals (potentially catalytic materials) were varied. The influence of hazes upon SO_2 oxidation was investigated under irradiated as well as dark conditions. The other series of experiments involved the production of clouds or fogs with natural microphysical features. The oxidation of SO_2 was observed in this system for irradiated and dark conditions and the influences of SO_2 concentration and heavy metal concentration were studied.

HAZE AND FOG GENERATION

The production of light hazes was accomplished by humidification of the chamber to near 100% relative humidity using a commercial nebulizer located at the top of the chamber; after humidification, all particulates were removed by absolute filters. The filtration process usually resulted in a decrease of relative humidity to about 90%. Subsequently, an aqueous solution containing given amounts of NaCl and heavy metals was nebulized by a Collison nebulizer using particle-free nitrogen as a carrier gas. Approximately one hour of nebulization was required to produce the desired concentrations of aerosol within the chamber. Following characterization of the aerosol, SO_2 ($\sim$1 ppm) and eventually NH_3 were added to the system. Filter samples were taken prior to the addition of SO_2 and regularly thereafter to determine the rate of catalytic oxidation of SO_2. The heated sampling inlet at a temperature of 70°C was used to eliminate the liquid water from the filter and, consequently, reduce artifact sulfate formation resulting from catalytic oxidation of SO_2 on the filter surface. Denser hazes were formed during pre-fog activities discussed below

The fogs required for in-fog experiments were produced in the smog chamber by expansion of near-saturated air. Initially, the chamber was humidified to near-saturated conditions by wetting the entire inner surfaces with distilled water using a remotely-controlled spray nozzle. With the relative humidity in the chamber typically in excess of 95% following the washdown, the desired nuclei were nebulized into the chamber to serve as condensation sites for fog formation.* As an inevitable consequence of the presence of large concentrations of hygroscopic nuclei and high pre-fog humidities, dense hazes (b_{scat} of about $4 \times 10^{-4} m^{-1}$) were formed during the pre-fog experiments. The measurements of catalytic oxidation of SO_2 in dense haze were made under these conditions.

*An absolute filtration system as well as an activated charcoal filter system are available to remove ambient aerosols or gases from the chamber prior to the preparation of the chamber for fog formation.

Subsequently, the chamber was pressurized to about 2.9 kilopascals (30 cm of water) relative to atmospheric pressure. The pressurized state was maintained for about 15 minutes to restore equilibrium temperature conditions and permit further evaporation from the wet chamber walls. Immediately after this waiting, pressure was decreased within the chamber by withdrawing air at a metered rate. Initially, the pressure was dropped abruptly to produce a state of supersaturation which activated the fog nuclei and secured the desired growth of the fog droplets. A continuous pressure reduction was required to maintain the fog by negating the effects of heating from the warm chamber walls.

While fogs have been sustained for periods longer than one hour in the chamber, their microphysical characteristics (i.e., liquid water content, drop sizes, and visibility) change appreciably over such long intervals. The fogs produced for these experiments were maintained for only 25 minutes. At the end of the 25-minute expansion period the pressure inside the chamber was generally about 2.9 kilopascals (30 cm of water) less than atmospheric pressure. At this point the fog was rapidly dissipated by allowing outside air to pass through the absolute filters and into the chamber, restoring atmospheric pressure. The resulting dilution from the increase in pressure was less than 3%. This procedure resulted in a fog of relatively uniform microphysical characteristics throughout its abbreviated duration. (The exception was the irradiated fogs. Due to heating effects, irradiated fogs tended to dissipate much sooner than fogs which were not irradiated.)

Measured haze, pre-fog haze, and fog characteristics are presented along with SO_2 oxidation data in the appropriate sections.

HAZE EXPERIMENTS

The catalytic oxidation of SO_2 was studied in two separate groups of light haze experiments as well as one series of dense pre-fog hazes. Each group of experiments is discussed separately below.

Nonirradiated Haze Experiments

A matrix of experiments was performed to determine the rate of catalytic oxidation of SO_2 in solution droplets smaller than 2 μm diameter with a

catalyst concentration of about 10^{-4}M or less. SO_2 concentrations of about 1.0 ppm were used for these experiments. Specific catalytic materials used included ferric chloride hexahydrate ($FeCl_3 \cdot 6H_2O$), manganese dichloride tetrahydrate ($MnCl_2 \cdot 4H_2O$), and vanadyl sulfate dihydrate ($VOSO_4 \cdot 2H_2O$). These materials were introduced into the chamber by nebulizing an aqueous solution of the catalytic material and a supporting electrolyte (NaCl) with a Collison nebulizer. The aerosol formed by these hygroscopic materials is composed of solution droplets smaller than 2.0 μm in diameter for relative humidities in the chamber of about 90% (see Figure 9).

The complete log of the 22 light haze experiments performed during this phase of the effort is presented in Table 6. The parameters shown for each haze experiment in Table 6 include: (1) The experiment title; (2) The concentration of SO_2 in parts per million; (3) Relative humidities, RH; (4) The Aitken nucleus concentration (per cubic centimeter); (5) Maximum b_{scat} in $10^{-4}m^{-1}$; and (6) The rate of SO_2 oxidation, R_{SO_2}, in percent per hour as determined by XRF analysis of filter samples acquired at about 30-minute intervals during the experiments. Except for experiments 1 and 2, the tests are classified in Table 6 according to the concentration of NaCl and heavy metal catalyst contained in the aqueous solution before nebulization. Experiment 1 involved only natural rural air and nuclei; experiment 2 involved only NaCl nuclei in the absence of catalyst.

Two distinct "haze" aerosols were generated during the series of experiments. Aerosol characteristics were controlled by altering the concentration of the supporting electrolyte (10^{-2} and 10^{-3}M NaCl) in the aqueous solution which was nebulized. Typical parameters of the two aerosol distributions responsible for the two haze types are exhibited in Figure 8. The resulting cumulative size distributions are shown in Figure 9. The two aerosol spectra presented in Figure 9 correspond to the aerosols observed early in experiments #8 and #16 listed in Table 6. The figure reveals the resulting increase in mean particle size due to the increased concentration of NaCl in the nebulizer solution. Values of b_{scat} as determined by an integrating nephelometer were found to be about 2.3 and 1.2 x $10^{-4}m^{-1}$ for the hazes nebulized from given quantities of aqueous solutions of 10^{-2} and 10^{-3}M NaCl, respectively.

TABLE 6

HAZE EXPERIMENTS

EXPERIMENT	SO_2 (ppm)	RH	AITKEN NUCLEI per cm^3	MAX. b_{scat} ($10^{-4}m^{-1}$)	R_{SO_2} (% hr^{-1})
1. NATURAL NUCLEI	1.0	89%	2.3×10^4	–	*
2. 10^{-2}M NaCl	0.7	90%	5.7×10^4	2.42	*
3. 10^{-2}M NaCl, 10^{-7}M $FeCl_3$	0.5	87%	4.3×10^4	2.09	*
4. 10^{-2}M NaCl, 10^{-7}M $FeCl_3$ + NH_3 (~10 ppb)	0.4	86%	3.7×10^4	1.92	*
5. 10^{-2}M NaCl, 10^{-7}M $MnCl_2$	0.6	87%	5.2×10^4	2.30	*
6. 10^{-2}M NaCl, 10^{-7}M $MnCl_2$ + NH_3 (~10 ppb)	0.4	85%	3.5×10^4	1.77	*
7. 10^{-2}M NaCl, 10^{-7}M $VOSO_4$	0.5	93%	6.0×10^4	2.71	*
8. 10^{-2}M NaCl, 10^{-7}M $VOSO_4$ + NH_3 (~10 ppb)	0.3	90%	3.5×10^4	2.56	*
9. 10^{-2}M NaCl, 10^{-7}M $VOSO_4$	0.5	89%	5.0×10^4	2.09	*
10. 10^{-2}M NaCl, 10^{-7}M $VOSO_4$ + NH_3 (~10 ppb)	0.3	92%	3.2×10^4	2.56	*
11. 10^{-2}M NaCl, 10^{-7}M $FeCl_3$	0.8	91%	5.1×10^4	2.88	~ 0.01
12. 10^{-2}M NaCl, 10^{-7}M $FeCl_3$ + NH_3 (~10 ppb)	0.5	93%	3.1×10^4	2.88	*
13. 10^{-2}M NaCl, 10^{-7}M $MnCl_2$	0.5	90%	5.2×10^4	2.71	*
14. 10^{-2}M NaCl, 10^{-7}M $MnCl_2$ + NH_3 (~1 ppm)	0.3	90%	3.3×10^4	2.88	~ 0.09
15. 10^{-3}M NaCl, 10^{-7}M $MnCl_2$	0.5	95%	2.4×10^4	1.15	*
16. 10^{-3}M NaCl, 10^{-7}M $MnCl_2$ + NH_3 (~1 ppm)	0.7	96%	2.0×10^4	1.59	*
17. 10^{-3}M NaCl, 10^{-7}M $FeCl_3$	1.0	93%	2.4×10^4	1.10	0.04
18. 10^{-3}M NaCl, 10^{-7}M $FeCl_3$ + NH_3 (~1 ppm)	0.8	93%	2.0×10^4	2.09	*
19. 10^{-2}M NaCl, 10^{-7}M $MnCl_2$	0.6	86%	6.0×10^4	2.88	*
20. 10^{-2}M NaCl, 10^{-7}M $MnCl_2$ + NH_3 (~1 ppm)	0.5	88%	4.0×10^4	2.88	*
21. 10^{-2}M NaCl	0.6	91%	5.2×10^4	3.84	*
22. 10^{-2}M NaCl + NH_3 (~1 ppm)	0.3	91%	3.9×10^4	3.29	~ 0.10

*NOT DETECTABLE

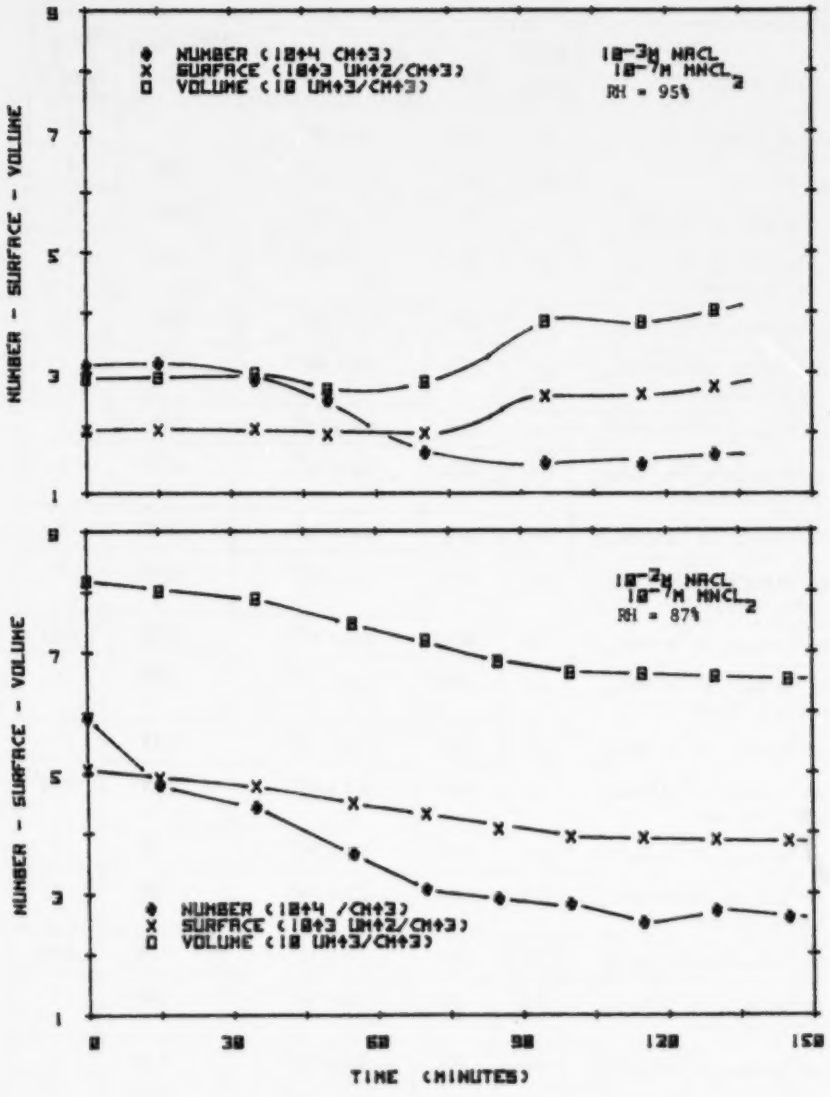

Figure 8. Parameters for Hazes Nebulized from Aqueous Solutions Containing 10^{-3}M and 10^{-2}M NaCl

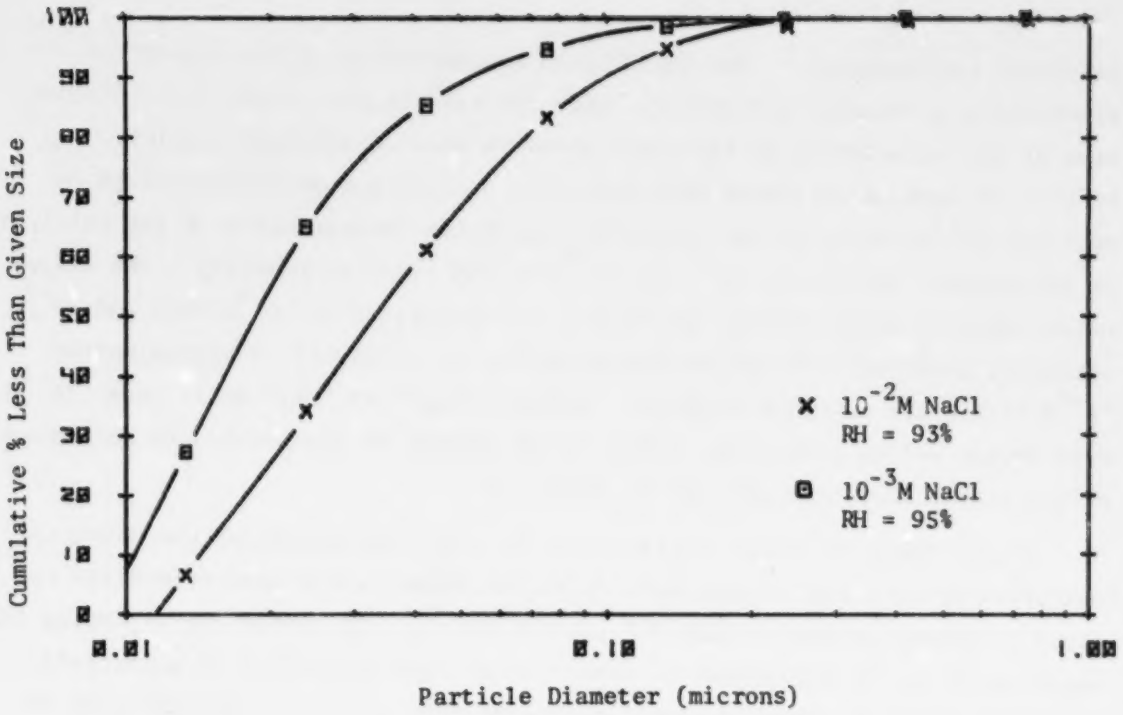

Figure 9. Cumulative Size Distributions for Hazes Nebulized from Aqueous Solutions Containing 10^{-3}M and 10^{-2}M NaCl for Specified Relative Humidities.

The concentration of catalyst in the haze droplets is dependent upon the initial concentrations of the catalyst and the supporting electrolytes in the nebulized droplets and upon ambient relative humidity. With the procedure used, droplets nebulized from the initial solution evaporate until the increasing concentration of the supporting electrolyte (NaCl) decreases the equilibrium vapor pressure of the droplet to the same value as that of its

immediate surroundings.* The equilibrium concentration of the supporting electrolyte is readily calculated. (See for example Low (1969) for a discussion of the calculation of the vapor pressure above a solution droplet). Results of such calculations show that, for initial concentrations of 10^{-2}M NaCl and 10^{-7}M catalyst, the expected equilibrium concentration of the catalyst in the aerosol is between 10^{-5} and 10^{-4}M at 90% relative humidity. The alternative mixture used, containing initial concentrations of 10^{-3}M NaCl and 10^{-7}M catalyst, produces equilibrium concentrations of catalysts of approximately 10^{-4}M within the solution droplets. Concentrations of heavy metal ions $< 10^{-4}$M were target values since they appear to be typical of concentrations occurring within clouds formed in parcels of urban air.**

In an effort to obtain qualitative, in situ information of the catalytic oxidation of SO_2, one of Calspan's diffusion chambers was used to monitor the cloud condensation nuclei (CCN)*** concentration. The reason for employing the measurement is the dependence of the critical supersaturation of a particle (supersaturation at which a particle attains free growth) on the dry size of the particle. As a result of catalytic oxidation of SO_2 within the solution droplets, the dry sizes of the particles are expected to increase with time. Therefore, an increase in the number of particles activated at a particular supersaturation is expected; this increase is attributable to those particles whose dry size was increased beyond the critical size by the addition of sul-

*For radii <0.1 μm, the increase in vapor pressure due to the decreased radius of curvature of the droplet may become significant. This effect is described by the Kelvin equation.

**Typical concentrations of Fe and Mn appear to be near 1 and 0.1 $\mu g/m^3$, respectively, in urban plumes (Georgii et al, 1974 and Flocchini et al, 1976). When these values are associated with LWC of about 0.1 g/m^3 as expected in clouds, the result is concentrations of about 10^{-4}M for Fe and 10^{-5}M for Mn.

***CCN are those particles whose unbounded growth due to the condensation of water vapor is initiated by low supersaturations (typically less than about 1%). As a result, CCN are the particles which are responsible for cloud and fog formation in the atmosphere.

furic acid. By setting the diffusion chamber at a fixed supersaturation and monitoring the number of nuclei activated as the oxidation process proceeds, the increase in the number concentration of CCN of a given critical size is obtained.

The CCN concentration measurements obtained from the diffusion chamber as functions of time for two typical experiments are shown in Figure 10. These data exhibit no consistent increase in the number of nuclei activated for the preset supersaturation level. The observed variation in concentration is within the approximate uncertainty range of the instrument. Calculations suggest that a rate of SO_2 oxidation on the order of 1%/hour would be necessary to produce clearly discernible results for the diffusion chamber technique. No such results were obtained.

Gases other than SO_2 were present at background levels only, and typical measured values were NO_x < 0.1 ppm, O_3 < 1 ppb, and THC ∿5 ppm. Ammonia was added during some of the experiments to assure that the acidity of the haze droplets was not inhibiting droplet absorption of SO_2. Since we presently have no convenient method for analyzing the amount of ammonia in the system, specific quantities of NH_3 were added volumetrically. During the first portion of the experiments, the quantity of NH_3 used was very small (∿10 ppb). In the later stages, sufficient NH_3 was added to achieve a 1 ppm concentration in the chamber. To obtain these concentrations, 6 and 600 ml, respectively, of gaseous NH_3 were introduced into the 590 m^3 chamber.

XRF analysis of filter samples acquired at regular intervals throughout these experiments reveal only minimal rates of SO_2 oxidation (see Table 6). Many of the samples contain no detectable levels of elemental sulfur, despite the fact that the samples were taken over a period of 2-1/2 hours. Sampling procedures used in this phase of the experiments, coupled with the detection limit of the XRF device, require quantities of about 0.4 $\mu g/m^3$ of sulfate for detection. For a 2-1/2 hour period, the collection of 1.2 $\mu g/m^3$ of sulfate (three times the detection limit) would represent a rate of about 0.02% hr^{-1} for an SO_2 concentration of 0.5 ppm. The results of observed R_{SO_2} listed in Table 6 indicate that maximum sulfate concentrations of about 1 $\mu g/m^3$ were only occasionally measured by the end of the experiments. Consequently, the

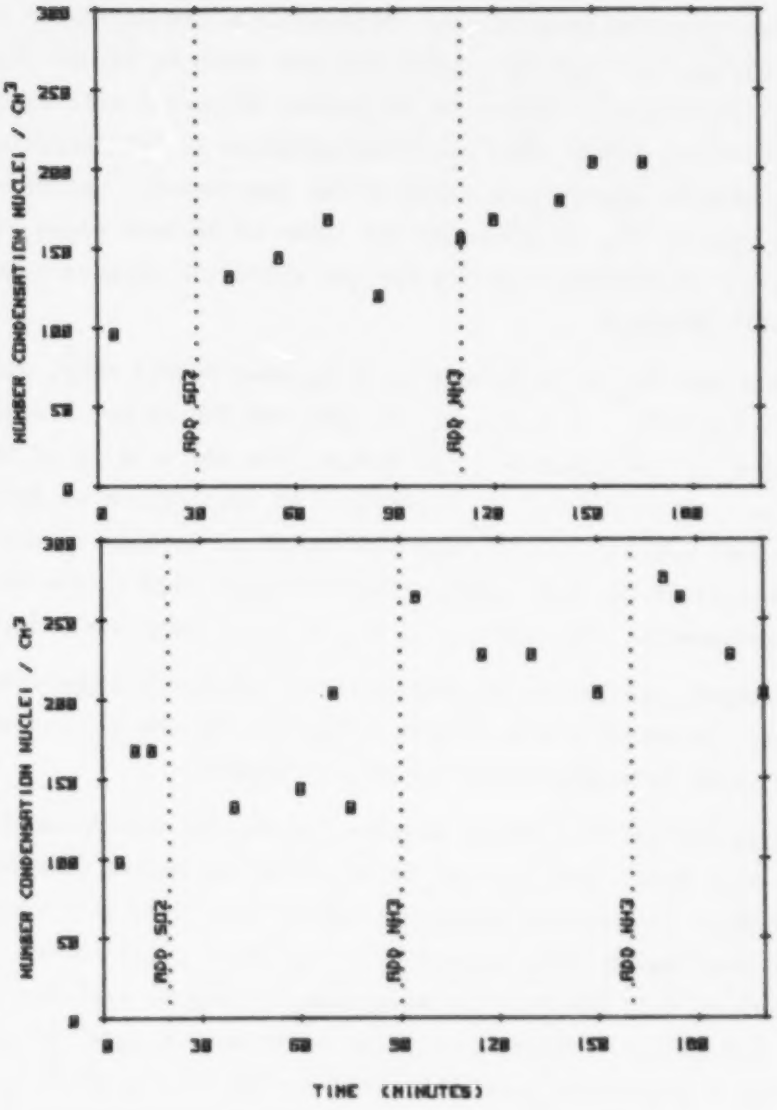

Figure 10. Typical Diffusion Chamber Data Showing CCN Concentration for 0.3% Supersaturation from Aerosols Produced by the Nebulization of an Aqueous Solution Containing 10^{-3}M and 10^{-2}M NaCl

results of these light haze experiments reveal consistent rates of SO_2 oxidation of $< 0.1\%\ hr^{-1}$, and in many tests there was no measurable sulfate formation, suggesting rates $< 0.01\%\ hr^{-1}$.

The dense haze measurements performed in conjunction with in-fog experiments #114, 115 and 116 present a somewhat different story. Data are presented in Table 7, which includes the following information: (1) The number of the pre-fog haze; (2) b_{scat} in $10^{-4}\ m^{-1}$; (3) Median SO_2 concentration in the haze in ppm; (4) The sulfate concentrations as measured prior to the addition of SO_2 and during the interval 15 to 30 minutes after SO_2 addition; (5) the concentrations within the chamber of Mn and Fe in $\mu g/m^3$ as determined by subsequent measurements of fog water samples; and, (6) The percent of available SO_2 apparently oxidized to produce the observed sulfate concentrations.

The concentrations of heavy metals contained in the solution droplets of these pre-fog hazes are conservatively estimated at values greater than $10^{-3}M$ and correspond to concentrations per unit volume of air (see Table 7) which are typical of the concentrations encountered in urban plumes (Georgii, et. al., 1974; and Flocchini, et. al., 1976). In contrast, concentrations of heavy metals in the previous haze experiments were less than $10^{-4}M$.

TABLE 7

SULFATE FORMATION IN PRE-FOG HAZES INDICATING DEPENDENCE ON HEAVY METALS

EXPT. NO.	b_{scat} ($10^{-4}m^{-1}$)	SO_2 (ppm)	SO_4 CONC BACKGROUND ($\mu g/m^3$)	SO_4 CONC AFTER SO_2* ADDITION ($\mu g/m^3$)	Mn ($\mu g/m^3$)	Fe ($\mu g/m^3$)	AVAILABLE SO_2 APPARENTLY OXIDIZED (NOT RATES)
114/1	12.45	1.0	3.09	11.19	0.1	<0.1	0.2%
115/1	19.19	0.5	4.63	31.64	1.0	<0.1	1.4%
116/1	24.24	0.75	3.47	81.02	1.0	1.0	2.6%

*MEASURED FROM T = 15 TO T = 30 MINUTES AFTER INTRODUCTION.

From the raw data it is apparent that SO_2 oxidation rates of the order of 0.5 to 5% per hour can occur in dense haze conditions. Because of the sparcity of available data, care must be taken in interpretation. The apparent dependence of R_{SO_2} on metal content of the haze is sufficiently large to be considered demonstrated. The functional dependence is hidden, however, by

changes in other parameters from experiment to experiment. The most important of these is probably the addition of the second metal catalyst in experiment #116. From data presented in the discussion of in-fog SO_2 oxidation in the next section, it is suspected that the change in liquid water content by a factor of two in the experiments may also be important.

Because of the known dependence of dissolution of SO_2 on pH of the solute it is suspected that the observed sulfate may have been produced very quickly after introduction of SO_2 and that R_{SO_2} was substantially diminished thereafter. If this apparent saturation of sulfate is correct, the most important data presented may be the total concentration of sulfate measured rather than the rate of production. Meaningful rate data, for wet plume model applications for example, require better time resolution in the experiments. The available data suggest that further experiments are warranted.

Irradiated Haze Experiments

A group of 12 haze experiments were performed to investigate the influence of hazes containing only trace quantities of heavy metals on the photooxidation of SO_2. These experiments are listed in Table 8. The parameters presented for each experiment include: (1) The experiment title; (2) An identifying number; (3) The concentrations in parts per million of sulfur dioxide (SO_2)*, total hydrocarbons (THC)**, methane (CH_4), total oxides of nitrogen (NO_x)***, nitric acid (NO)***, and ozone (O_3); (4) The median temperature in degrees Celsius; (5) The median relative humidity; (6) The number of Aitken nuclei per cubic centimeter at the beginning and end of each experiment; (7) The observed mean oxidation rate of SO_2 in percent per hour; and, (8) maximum b_{scat} in $10^{-4}m^{-1}$.

*Mean values

**Units are in parts per million carbon-ppmC

***Due to a malfunction of the NO_x-NO_2-NO analyzer, the lower recorded values of NO_x and NO are qualitative. To obtain the higher concentrations, NO was metered into the chamber, thus eliminating the reliance on the faulty gas analyzer.

Typically, each of the irradiated haze experiments exhibits a mean R_{SO_2} of a few tenths of a percent per hour which is in good agreement with the rate of SO_2 photooxidation in irradiated clean air systems observed by others (Kocmond and Yang, 1975; Kasahara and Takahashi, 1976). As noted earlier, this agreement between the rates of SO_2 oxidation observed in the irradiated haze experiments and the rates of SO_2 oxidation for irradiated clean air systems suggests that the total sulfate formed during the irradiated haze experiments was due to the same photooxidation mechanism responsible for sulfate formation in irradiated clean air tests. These results can be applied only to hazes containing trace concentrations of heavy metals. Other experimental data concerning fogs suggest similar conclusions.

TABLE 8
IRRADIATED HAZE EXPERIMENTS

EXPERIMENT	EXP. #	GAS CONCENTRATION – ppm					
		SO_2	THC*	CH_4	NO_x	NO	O_3
RURAL AIR (W/O NATURAL NUCLEI) + SO_2	101/3	0.45	2.6	1.9	$\leq$0.1	$\leq$0.1	0.002
RURAL AIR (W/O NATURAL NUCLEI) + SEA SALT NUCLEI + SO_2 + NH_3 (~1 ppm)	101/4	0.30	2.8	1.9	$\leq$0.1	$\leq$0.1	0.003
RURAL AIR	102/1	0.01	2.8	2.4	$\leq$0.1	$\leq$0.1	0.015
RURAL AIR + SO_2	102/2	1.00	2.3	1.8	$\leq$0.1	$\leq$0.1	0.030
RURAL AIR + SEA SALT NUCLEI	103/1	0.01	2.2	1.9	$\leq$0.1	$\leq$0.1	0.020
RURAL AIR + SEA SALT NUCLEI + SO_2	103/2	1.00	2.2	1.9	$\leq$0.1	$\leq$0.1	0.020
RURAL AIR	105/1	0.01	2.6	2.0	$\leq$0.1	$\leq$0.1	0.009
RURAL AIR + SO_2	105/2	0.50	2.6	2.0	$\leq$0.1	$\leq$0.1	0.011
RURAL AIR + SO_2 + NH_3 (~1 ppm)	105/3	0.20	2.6	2.0	$\leq$0.1	$\leq$0.1	0.001
RURAL AIR (W/O NATURAL NUCLEI)	111/1	0.04	5.8	3.9	$\leq$0.1	$\leq$0.1	0.010
RURAL AIR (W/O NATURAL NUCLEI) + PHOTOCHEMICAL AEROSOL + SO_2	111/2	1.00	5.8	3.9	$\leq$0.1	$\leq$0.1	0.020
RURAL AIR (W/O NATURAL NUCLEI) + PHOTOCHEMICAL AEROSOL + SO_2 + NO	111/3	5.00	5.8	3.9	20	20	$<$0.001

* ppmC

(continued)

TABLE 8 (continued)

EXP. #	T (°C)	RH	AITKEN NUCLEI #/cm^3 BEFORE/AFTER	CCN** #/cm^3 BEFORE/AFTER	R_{SO_2} % hr^{-1}	MAX. b_{scat} (10^{-4} m^{-1})
101/3	22	93%	$2.2\times10^4/9.5\times10^4$	1505/1700	0.2	3.2
101/4	24	85%	$9.5\times10^4/9.0\times10^4$	1700/1747	1.3	3.2
102/1	21	93%	$1.4\times10^4/1.2\times10^4$	516/576	*	2.4
102/2	24	94%	$2.0\times10^5/9.5\times10^4$	576/624	0.2	4.1
103/1	23	95%	$5.0\times10^4/3.0\times10^4$	960/1344	*	19.2
103/2	26	91%	$7.5\times10^5/1.0\times10^5$	1344/1404	0.2	12.1
105/1	24	94%	$\sim 700/8.0\times10^5$	20/40	*	<0.5
105/2	26	91%	$8.0\times10^5/1.5\times10^5$	40/1596	0.2	1.3
105/3	26	90%	$1.3\times10^5/9.0\times10^4$	1596/$>$3000	0.2	3.9
111/1	22	95%	$\sim 700/4.9\times10^4$	64/140	0.3	1.5
111/2	24	91%	$4.6\times10^4/1.8\times10^5$	140/164	0.1	2.9
111/3	26	86%	$1.3\times10^5/9.3\times10^4$	164/2840	0.1	12.1

* NOT DETECTABLE
**SUPERSATURATION = 0.45%

The one exception to the noted rates of SO_2 oxidation of a few tenths of a percent for the irradiated haze experiments are the results listed in experiment #101/4 in which a rate of oxidation greater than 1% hr^{-1} was observed. The results of this experiment, which is merely a continuation of experiment #101/3 with the exception that about 1 ppm of NH_3 has been added to the chamber, have not been substantiated with further experiments.

It is of interest to compare the observed SO_2 oxidation in the dense hazes to the photooxidation of SO_2 in clean air ($\sim$0.2% hr^{-1}). The sulfate formed in the #114/1 haze is about the same amount as would be produced in an irradiated clean air system during a one-hour period. An irradiated clean air system would require about 10 hours to produce the levels of sulfate observed in hazes #115/1 and 116/1. Thus, it appears that concentrations of heavy metals such as were used in these experiments and which are commonly found in urban plumes can potentially produce significant levels of SO_2 oxidation in dense haze situations.

Discussion of Results

Barrie and Georgii (1976) found the rate of SO_2 absorption in an aqueous system containing 10^{-5}M $MnCl_2$ to be given by

$$R = 1.11 \times 10^{-7} [SO_2]_g^{0.727} \quad (2)$$

where $[SO_2]_g$ is the gaseous concentration of SO_2 in ppb. The units of the rate are M/min. Based on one of our typical light haze experiments with an SO_2 concentration of 1 ppm and a volume of solution droplets of 8×10^{-5} ml/m^3, their expression results in 0.015 $\mu g/m^3$ of sulfate being produced in a 120 minute period (assuming that all of the absorbed SO_2 was oxidized to sulfate). The resultant SO_2 oxidation rate of about 10^{-4}% hr^{-1} is two orders of magnitude lower than the rates we are capable of resolving with our aerosol sampling-XRF analysis procedures. Consequently, unless SO_2 oxidation rates at least two orders of magnitude greater than those observed by Barrie et. al. were encountered in the nonirradiated hazes of this series

of experiments, we should not have expected to observe sulfate formation. To the point that we could detect little if any sulfate in these hazes, our results are consistent with those of Barrie et. al.

Cautiously, we can conjecture that the catalytic oxidation of SO_2 in non-irradiated light hazes such as these will be much less than 0.1% hr^{-1} and perhaps lower than 0.01% hr^{-1} and consequently will not significantly contribute to the total atmospheric oxidation of SO_2. However, it is possible that higher concentrations of these heavy metals (i.e., V, Mn, and Fe) or other catalytic materials of higher catalytic activity may produce substantially greater oxidation rates.

The following conclusions appear warranted:

1. The rate of catalytic oxidation of SO_2 in persistent hazes (droplet diameters < 2 μm) in the presence of ions of Mn or Fe at $< 10^{-4}$M is not significant (i.e., < 0.01% hr^{-1}) unless haze density is such as to reduce visibility to substantially less than 20 km.

2. No consistent discernible effect on SO_2 oxidation was observed by the addition of approximately 1 ppm NH_3 to light haze situations. This implies that the catalytic oxidation of SO_2 within the solution droplets was not quenched by the lack of dissolved SO_2 in the solution droplets.

3. Filter samples from dense pre-fog hazes (b_{scat} on the order of $10^{-2}m^{-1}$) revealed considerable sulfate formation. Within a 30-minute period, sulfate levels as high as 80 $\mu g/m^3$ were observed, corresponding to the oxidation of about 3% of the available SO_2 or an average R_{SO_2} of over 5% hr^{-1}. The sulfate formation appeared to be dependent upon the concentration of heavy metals.

4. Measured rates of SO_2 oxidation for irradiated hazes containing only trace concentrations of heavy metals agree well with rates of SO_2 oxidation observed for irradiated clean air systems. This agreement suggests that the observed sulfate formation in these irradiated haze experiments is due to the same photooxidation mechanism responsible for sulfate formation in irradiated clean air tests. No additional contribution due to the presence of the haze is discernible.

IN-FOG* EXPERIMENTS

A series of experiments aimed at assessing the oxidation of SO_2 in fogs with known microphysical characteristics, known concentrations of SO_2, and known concentrations of heavy metals was performed. A log of these experiments is shown in Tables 9 and 10. Some 28 separate experiments are displayed in this log along with significant experimental parameters. The two distinct groups within this matrix of experiments are (1) In-fog without irradiation (Table 9); and (2) In-fog with irradiation (Table 10). This grouping of experiments was chosen to elicit possible synergistic effects on the oxidation rate of SO_2 as a result of the simultaneous influence of the fog and irradiation.

The range of SO_2 concentrations used in this series of experiments was chosen to encompass the spectrum of conditions expected in such drastically different situations as clean remote locations ($\sim$10 ppb) and heavily polluted industrial plumes (>10 ppm). Specific interest was expressed by the EPA in the refinery to be built at Eastport, Maine, and the interaction of its stack emissions with the frequent coastal fogs experienced in that area. Based on expected emissions of 153.7 g/sec of SO_2 and 217 g/sec of NO_x**, the atmospheric diffusion of the plume under stable conditions and a wind speed of 1 m/sec was modeled. The resultant centerline concentrations in the plume 1 km downwind of the stack were selected as upper limit values for the in-fog experiments. The particular values for SO_2 and NO_x were about 10 ppm and 20 ppm, respectively.

*To avoid repetition, the term fog is applied to our chamber clouds exhibiting characteristics similar to natural fogs and clouds, the only difference between fogs and clouds being their proximity to the ground.

**These values of gaseous emissions are estimates furnished by Dr. Richard Keppler, Director or ORD of the EPA in Region 1, and Mr. Warren Peters also of EPA, Region 1.

TABLE 9
IN-FOG EXPERIMENTS

EXPERIMENT	EXP. #	T (°C)	GAS CONCENTRATIONS - PPM					
			SO_2	THC*	CH_4	NO_x	NO	O_3
RURAL AIR + SEA SALT NUCLEI	100/1	19	0.04	2.6	2.3	<0.1	<0.1	0.001
RURAL AIR + SEA SALT NUCLEI + SO_2	100/2	19	0.40	3.2	2.6	<0.1	<0.1	0.001
RURAL AIR (W/O NATURAL NUCLEI) + SEA SALT NUCLEI	101/1	19	0.02	2.5	1.9	<0.1	<0.1	<0.001
RURAL AIR (W/O NATURAL NUCLEI) + SEA SALT NUCLEI + SO_2	101/2	19	0.60	2.5	1.9	<0.1	<0.1	0.001
RURAL AIR + SEA SALT NUCLEI + SO_2	106/1	22	6.50	2.6	1.7	<0.1	<0.1	0.002
RURAL AIR + SEA SALT NUCLEI + SO_2	106/2	22	5.00	2.6	1.7	20.0	20.0	0.001
RURAL AIR + PHOTOCHEMICAL AEROSOL + SO_2	110/1	22	0.80	2.6	1.8	<0.1	<0.1	0.010
RURAL AIR (W/O NATURAL NUCLEI) + SEA SALT NUCLEI + SO_2	112/1	22	1.10	6.1	3.8	<0.1	<0.1	0.001
RURAL AIR (W/O NATURAL NUCLEI) + SEA SALT NUCLEI + SO_2	112/3	22	6.00	6.1	3.8	<0.1	<0.1	<0.001
RURAL AIR + SEA SALT NUCLEI + 10^{-2} M $MnCl_2$ + SO_2	114/1	17	0.60	3.2	2.2	<0.1	<0.1	0.001
RURAL AIR + SEA SALT NUCLEI + 10^{-2} M $MnCl_2$ + SO_2	114/2	18	0.90	3.2	2.2	<0.1	<0.1	0.001
RURAL AIR + SEA SALT NUCLEI + 10^{-1} M $MnCl_2$ + SO_2	115/1	18	0.30	15.0	>10	<0.1	<0.1	<0.001
RURAL AIR + SEA SALT NUCLEI + 10^{-1} M $MnCl_2$ + SO_2	115/2	18	0.80	15.0	>10	<0.1	<0.1	<0.001
RURAL AIR + SEA SALT NUCLEI + 10^{-1} M $MnCl_2$ + SO_2 + SOOT	115/4	19	0.70	25.0	>10	<0.1	<0.1	<0.001
RURAL AIR + SEA SALT NUCLEI + 10^{-1} M $FeCl_3$ + 10^{-1} M $MnCl_2$ + SO_2	116/1	18	0.40	13.0	>10	<0.1	<0.1	<0.001
RURAL AIR + SEA SALT NUCLEI + 10^{-1} M $FeCl_3$ + 10^{-1} M $MnCl_2$ + SO_2	116/2	18	1.0	13.0	>10	<0.1	<0.1	<0.001

*ppmC

(continued)

TABLE 9 (continued)

EXP. #	AITKEN NUCLEI #/cm^3 BEFORE/AFTER	CCN* #/cm^3		ml OF FOG WATER COLLECTED	MAX. b_{scat} ($10^{-4}m^{-1}$)
		PRE FOG	POST FOG		
100/1	–	1824	1608	10.0	1354
100/2	–	1552	1152	10.0	1279
101/1	$3.2x10^4/2.4x10^4$	2136	1260	10.0	1096
101/2	$2.2x10^4$/ --	1260	984	9.8	1047
106/1	$4.1x10^4/3.1x10^4$	1152	996	10.7	1151
106/2	$2.9x10^4/2.3x10^4$	1044	780	10.1	1096
110/1	$9.4x10^4/9.2x10^4$	2712	2832	7.3	1535
112/1	$5.3x\ 10^4/3.6x10^4$	1456	1464	10.5	1212
112/3	$2.6x10^4/2.3x10^4$	1480	1376	6.6	886
114/1	$4.8x10^4/3.1x10^4$	2136	1536	9.0	1151
114/2	$3.0x10^4/2.4x10^4$	1632	1092	9.1	980
115/1	$4.0x10^4/3.2x10^4$	1896	1644	8.5	1279
115/2	$2.6x10^4/2.4x10^4$	1944	1788	8.2	1279
115/4	$2.2x10^4/1.8x10^4$	2340	1536	8.6	1316
116/1	$5.4x10^4/3.7x10^4$	2272	1908	8.1	1316
116/2	$3.1x10^4/2.5x10^4$	2040	1904	7.2	1151

*SUPERSATURATION = 0.45%

TABLE 10 IRRADIATED IN-FOG EXPERIMENTS

EXPERIMENT	EXP. #	T (°C)	GAS CONCENTRATIONS - PPM					
			SO_2	THC*	CH_4	NO_x	NO	O_3
RURAL AIR + SEA SALT NUCLEI	104/1	24	0.04	2.8	2.4	<0.1	<0.1	0.025
RURAL AIR + SEA SALT NUCLEI +SO_2	104/2	26	0.70	2.8	2.4	<0.1	<0.1	0.015
RURAL AIR + SEA SALT NUCLEI + SO_2	107/1	21	5.80	2.0	1.7	<0.1	<0.1	0.001
RURAL AIR + SEA SALT NUCLEI + SO_2 + NO	107/2	22	4.80	2.0	1.7	20.0	20.0	<0.001
RURAL AIR + SEA SALT NUCLEI + SO_2	108/1	19	5.30	4.6	3.9	<0.1	<0.1	0.001
RURAL AIR + SEA SALT NUCLEI + SO_2	108/2	20	3.50	4.6	3.9	<0.1	<0.1	0.001
RURAL AIR + SEA SALT NUCLEI + SO_2	108/3	21	2.50	4.6	3.9	<0.1	<0.1	0.004
RURAL AIR + SEA SALT NUCLEI + SO_2 + NO	108/4	20	4.50	4.6	3.9	20	20	<0.001
RURAL AIR (W/O NATURAL NUCLEI) + SEA SALT NUCLEI + SO_2	112/2	21	0.40	6.1	3.8	<0.1	<0.1	<0.001
RURAL AIR (W/O NATURAL NUCLEI) + SEA SALT NUCLEI + SO_2	112/4	21	4.40	6.1	3.8	<0.1	<0.1	<0.001
RURAL AIR + SEA SALT NUCLEI + 10^{-2} M $MnCl_2$ + SO_2	114/3	19	1.10	3.2	2.2	<0.1	<0.1	0.002
RURAL AIR + SEA SALT NUCLEI 10^{-2} M $MnCl_2$ + SO_2	115/3	19	1.50	15.0	>10	<0.1	<0.1	0.002

*ppmC

(continued)

TABLE 10 (continued)

EXP.#	AITKEN NUCLEI #/cm^3 BEFORE/AFTER	CCN* #/cm^3 PRE FOG	CCN* #/cm^3 POST FOG	ml OF FOG WATER COLLECTED	MAX. b_{scat} ($10^{-4}m^{-1}$)
104/1	$7.4x10^4/5.0x10^4$	1464	1128	4.5	781
104/2	$4.4x10^4/1.0x10^5$	1188	1020	3.3	279
107/1	$5.5x10^4/1.0x10^5$	1088	2730	5.8	1123
107/2	$9.0x10^4/8.2x10^4$	2840	4000	4.5	1096
108/1	$5.2x10^4/8.5x10^4$	1200	1248	5.5	853
108/2	$5.4x10^4/7.5x10^4$	1272	1416	0.8	59
108/3	$6.5x10^4/6.2x10^4$	1656	2304	2.3	512
108/4	$4.2x10^4/4.0x10^4$	2568	2832	7.5	1096
112/2	$3.0x10^4/2.6x10^4$	1824	1760	5.4	622
112/4	$2.8x10^4/4.0x10^5$	1008	2264	3.1	79
114/3	$2.4x10^4/7.4x10^4$	1188	1800	3.0	171
115/3	$2.4x10^4/2.6x10^4$	1308	1760	4.3	658

*SUPERSATURATION = 0.45%

The parameters for each in-fog experiment listed in Tables 9 and 10 are: (1) An identifying number; (2) The median temperature in degrees Celsius; (3) The concentrations in parts per million of sulfur dioxide (SO_2)* , total hydrocarbons (THC) **, methane (CH_4) total oxides of nitrogen (NO_x)*** , nitric oxide (NO)*** , and ozone (O_3): (4) The number of Aitken nuclei and cloud condensation nuclei (CCN) per cubic centimeter before and after each fog event; (5) The volume of liquid water in milliliters col ected during the fog; and (6) The maximum b_{scat} in $10^{-4} m^{-1}$ as determined from measurements of visibility with an optical transmissometer (b_{scat} = 3.91/visibility (meters)).

The aerosols used in these experiments as condensation nuclei for the fogs consisted primarily of NaCl. They were generated by the nebulization of a commercial mixture of sea water**** which contained even the trace elements normally found in the sea. In specific experiments, the aerosol normally found in the rural, western New York air were also allowed to remain during the fog.

For nine of the in-fog experiments (#114-116 series) the nebulizer solution used to generate nuclei for the experiments was doped with manganese dichloride tetrahydrate ($MnCl_2 \cdot 4H_2O$). In two of these nine experiments (#116 series) ferric chloride hexahydrate ($FeCl_3 \cdot 6H_2$)) was also added to the nebulizer solution. The concentration of these compounds in the nebulizer solution is presented in Tables 9 and 10 for each experiment. In experiment #115/4, about 10 grams of soot scraped from the flue of a local wood burning fireplace was disseminated as a fine powder into the chamber. These nine experiments were aimed at assessing the role of increased concentrations of heavy metals upon the in-fog oxidation of SO_2.

---

*Mean values

**Units are parts per million carbon - ppmC

***Due to a malfunction of our NO_x-NO_2-NO gas analyzer, the low reported values (i.e., < 0.1) of NO_x and NO are only qualitative. The higher concentrations were obtained when NO was actually metered into the chamber, thus eliminating the reliance upon the faulty gas analyzer.

****The mixture is Instant Ocean and is distributed by Aquariums Systems, Inc. 33208 Lakeland Blvd., Eastlake, OH 44094.

Fogs in Tables 9 and 10 which exhibit the same series number (i.e., #112/1, 112/2, and 112/3 - where 112 is the series number) are consecutive fogs produced in the same air and aerosol sample at roughly two hour intervals. During the interim period, two filter samples were obtained and the previously collected fog water removed from the chamber. Typically, only the SO_2 concentration was altered between fogs, but occasionally nitric oxide was added. In one instance (between fogs #115/4 and 115/3) about 10 g of dry soot nuclei were added to the chamber.

The fogs were characterized by measurements of visibility, liquid water content (LWC), and number and size distributions of fog droplets. An example of the time history of the microphysical characteristics on one of the non-irradiated fogs (#100/1) is shown in Figure 11. Droplet spectra are shown for selected times during the fog. The legend of each size distribution includes: (1) The age of the fog, T, in minutes: (2) Mean radius of the fog droplets, R, in microns; (3) Total number of fog droplets per cm^3, N; (4) Liquid water content, W, in grams per m^3; and (5) Visibility in meters, V, as calculated from the measured drop distribution. All of these values are based upon the measured size distribution of the fog droplets discussed below.

Common trends in microphysical properties of these fogs can be noted in the plots in the middle and at the bottom of Figure 11. As shown by the data, soon after initiation of the fog, visibility rapidly drops to its lowest value. The decrease in visibility is the result of the appearance of a large number of small droplets. With age, visibility improves due to the selective growth of the large water droplets (at the expense of smaller droplets) and their eventual loss from the system due to sedimentation, thus decreasing the total amount of light scattered. The loss of droplets by sedimentation is also indicated by the decreasing LWC of the fog as well as total number of fog droplets, even though the mean size of the droplets is increasing.

The fog microphysics data were obtained by collection of fog droplets by impaction on a glass slide coated with a thin film of gelatin. The resulting craters in the gelatin have been found to be almost exactly twice the diameter of the initial droplet, thus providing a measure of true drop diameter. In

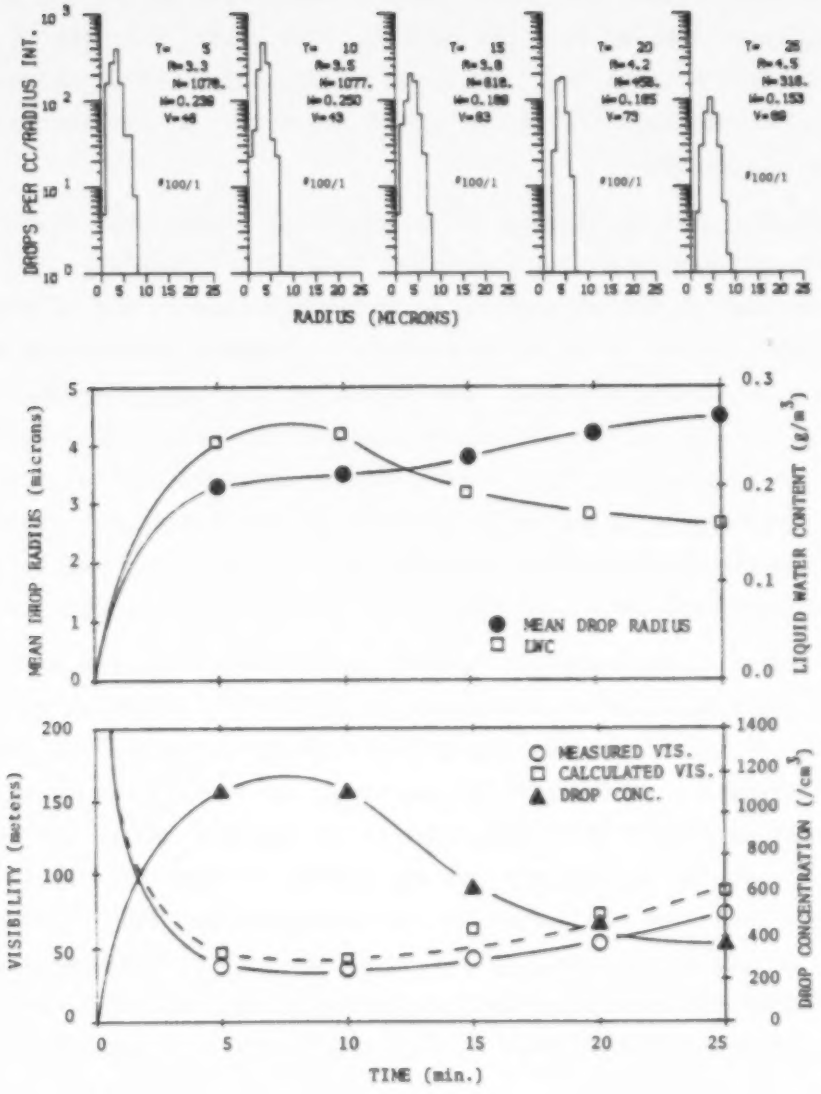

Figure 11. Microphysical Characteristics of Fog #100/1 As Functions of Time

addition, the characteristics of the impactor are such that the collection efficiency is acceptable even for one micron diameter droplets. As a result of known exposure time of the slide, measurement of the size spectra includes a determination of concentration as well as sizes of the fog droplets from which LWC can be computed. Due to the effort required to determine the droplet spectra (i.e., counting and sizing of ∿200 craters per spectra) of the fogs, the droplet size distributions of only eight of the fogs are presented. These data are summarized in Table 11 and additional details may be found in Appendix A. As shown by Table 11, fog characteristics are quite consistent within the two groupings and comparable to those of natural fogs. The parameters presented in Table 11 for each fog are the fog number or description, the mean values of fog droplet radius (μm), droplet concentration (#/cm^3), and LWC (g/m^3), and the maximum b_{scat} ($10^{-4}m^{-1}$).

TABLE 11 MEAN FOG MICROPHYSICAL PROPERTIES

	FOG #	MEAN RADIUS (μm)	DROP CONCENTRATION (#/cm^3)	LWC (g/m^3)	MAX. b_{scat} ($10^{-4}m^{-1}$)
W/O IRRADIATION	100/1	3.9	700	0.20	1071
	100/2	3.6	750	0.16	869
	101/1	4.0	600	0.21	1001
	101/2	3.7	650	0.14	755
	116/1	3.8	600	0.19	959
	116/2	3.2	500	0.10	485
W/IRRADIATION	107/1	3.3	900	0.19	1023
	107/2	2.7	800	0.08	755
NATURAL FOGS					
	RADIATION FOG (INLAND)*	5.0	200	0.11	461
	ADVECTION FOG (COASTAL)*	10.0	40	0.17	154

*JIUSTO, 1964

Visibility determinations are obtained from measurements of the extinction of a beam of white light traversing twice the diameter of the chamber (~18 m) and calculated from measured drop size distributions. Both the measured and calculated visibilities are displayed in the characterizations presented in Figure 11. The visibilities presented in Appendix A are calculated values based upon measured size distributions.

The LWC of a fog was determined by two methods. For the collection of samples of fog water, the Calspan Fog Water Collector is placed in the chamber and removes the droplets from a known volume of air. The droplets are removed by impaction upon a glass column from which they drip into a glass collection bottle. Comparison of the volume of liquid water collected to the volume of air sampled results in a measure of the average LWC of the fog as well as a sample of fog water suitable for chemical analysis. Another determination of LWC may be obtained by integration of the droplet size distributions. The latter method was used to provide the values of LWC displayed in Figure 11 and in Appendix A.

Determinations of SO_2 oxidation occurring within the fogs were accomplished by two independent means. The aforementioned Fog Water Collector was operated during the last 15 minutes of each fog, collecting a sample of fog water. These fog water samples represented an average over the last 15 minutes of the fog and generally consisted of about 10 ml of fog water. The pH of the fog water samples was measured immediately after each fog with a microelectrode. Subsequently, portions of the samples were sent to RTP for analysis by ion chromatography, and portions were retained for analysis (at Calspan) of heavy metal content by atomic absorption. The sulfate content of the fog water as measured by ion chromatography provided a means for the determination of SO_2 oxidation.

In addition to samples of fog water, filter samples were acquired before and after each fog using the technique described at the conclusion of Section 5. The sulfuric acid present on these samples was then fixed in an atmosphere of NH_3 (for stabilization), and the samples were mailed to RTP for subsequent analysis by XRF. Assuming that all of the elemental sulfur measured by XRF analysis existed on the filter in the form of a sulfate, a second, independent determination of SO_2 oxidation was available.

Results

The results of various analyses of the filter and water samples collected for each fog event are presented in Table 12. This table displays: (1) The identifying number of the fog; (2) The measured pH of the fog water sample; (3) The average liquid water content of the fog in g/m^3 as determined by the fog water collector; (4) Status of irradiation (I implies an irradiated fog; - implies a nonirradiated fog); (5) Pre-fog b_{scat} in $10^{-4}m^{-1}$; (6) Median SO_2 concentration in ppm; (7) Nitrate and sulfate concentrations of the collected fog water in μg/ml from analysis by ion chromatography; (8) Sulfate concentrations in $\mu g/m^3$ as determined by XRF analysis of filter samples acquired before and after the fog; (9) The concentrations of Na and Cl in $\mu g/m^3$ as determined by XRF analysis of filter samples obtained before and after the fog; and (10) The concentrations in μg/ml of Mn, Mg, Cu, and Fe as well as their total concentration in the collected fog water as determined by atomic absorption. Missing data points generally indicate an insufficient quantity of sample for a complete analysis.

Although the potential importance of the nitrate content of the collected fog water is recognized, this variable was not emphasized during the experiments and hence discussions of the data will concentrate on sulfates.

The most significant data from the in-cloud experiments stems from analyses of the collected fog water. Measured values of the pH of the collected fog water were typically about 3. Such values are in fair agreement but generally lower than field measurements of the pH of precipitation events in the northeastern United States (e.g., Likens, 1976).

Comparison of the sulfate content of the collected fog water from nonirradiated experiments suggests a dependence of the sulfate concentration in the fog water on the SO_2 concentration during the experiment. The correlation of sulfate formation with SO_2 concentration is most clearly demonstrated by the data shown in Figure 12 where the observed fog water sulfate concentrations are plotted as functions of median SO_2 concentrations for the nonirradiated fog experiments. The two types of data points (solid and open symbols) represent data from experiments where additional heavy metals (Mn and Fe) were and

TABLE 12 CHEMISTRY OF IN-FOG EXPERIMENTS

FOG #	pH	LWC (g/m^3)	IRRAD. OF FOG	PRE-FOG b_{scat} ($10^{-4} m^{-1}$)	SO_2 (ppm)	NITRATE CONC. ($\mu g/m\ell$)	SULFATE CONC. ($\mu g/m\ell$)	SULFATE CONC. ($\mu g/m^3$)	
							FOG WATER	PRE-FOG	POST-FOG
100/1	4.3	0.35	–	–	0.04	0.84	14.16	8.88	3.86
100/2	4.3	0.35	–	–	0.40	0.73	31.70	4.63	4.63
101/1	3.0	0.35	–	15.4	0.02	0.004	4.49	1.93	0.39
101/2	1.5*	0.35	–	4.1	0.60	0.045	15.45	–	–
104/1	3.5	0.16	I	15.9	0.04	–	24.26	10.04	4.25
104/2	–	0.12	I	8.2	0.70	6.48	42.76	4.63	6.17
106/1	2.2	0.38	–	12.1	6.50	–	68.83	7.33	4.25
106/2	2.8	0.36	–	17.1	5.00	7.83	70.61	5.79	6.56
107/1	2.4	0.21	I	15.9	5.80	–	–	8.88	62.90
107/2	2.1	0.16	I	32.9	4.80	219.60	–	50.94	62.52
108/1	1.0*	0.20	I	13.5	5.30	14.23	102.10	13.12	10.42
108/2	1.5*	0.03	I	9.0	3.50	3.69	142.80	10.81	15.05
108/3	1.0*	0.08	I	4.8	2.50	2.07	251.70	15.05	20.84
108/4	2.4	0.27	I	9.6	4.50	54.31	232.80	20.84	27.40
110/1	2.8	0.26	–	3.7	0.80	7.01	49.83	22.38	29.33
112/1	3.1	0.37	–	32.9	1.10	7.81	76.54	13.89	2.32
112/2	2.7	0.19	I	15.9	0.40	15.37	43.85	3.09	3.86
112/3	2.6	0.23	–	6.9	6.00	11.33	190.70	15.82	2.70
112/4	2.6	0.11	I	2.6	4.40	0.37	9.43	2.70	20.07
114/1	3.6	0.32	–	12.4	0.60	–	35.99	11.19	8.49
114/2	3.6	0.32	–	3.6	0.90	0.33	28.09	10.03	6.95
114/3	3.35	0.11	I	2.9	1.10	1.99	37.75	5.79	8.88
115/1	3.9	0.30	–	19.2	0.30	–	85.02	31.64	18.14
115/2	3.4	0.29	–	9.2	0.80	–	72.72	14.28	10.81
115/3	3.15	0.15	I	2.4	1.50	0.648	82.96	10.42	13.51
115/4	3.9	0.30	–	8.7	0.70	–	73.92	44.76	9.65
116/1	2.6	0.29	–	24.2	0.40	–	359.32	81.04	65.60
116/2	2.65	0.26	–	14.4	1.00	–	284.83	57.89	50.17

*POSSIBLE INSTRUMENT ERROR

(continued)

TABLE 12 (continued)

	SUPPORTING ELECTROLYTE ($\mu g/m^3$)				FOG WATER ($\mu g/ml$)				
FOG #	Na:PRE	Na:POST	Cl:PRE	Cl:POST	Mn	Mg	Cu	Fe	TOTAL
100/1	4.24	1.16	12.47	2.96	<0.004	0.403	0.025	0.046	0.48
100/2	1.54	1.03	2.96	1.41	<0.004	0.224	0.035	0.007	0.27
101/1	5.27	2.19	18.00	5.14	<0.004	0.525	0.004	<0.004	0.54
101/2	2.19	1.16	4.12	1.93	<0.004	0.242	0.053	0.004	0.30
104/1	5.27	1.41	19.03	6.59	–	–	–	–	–
104/2	1.80	1.93	7.20	3.73	–	–	–	–	–
106/1	2.70	1.54	2.96	2.31	<0.004	0.513	0.190	0.057	0.76
106/2	1.29	1.03	2.31	0.33	<0.004	0.166	0.627	0.334	1.13
107/1	3.09	1.24	12.22	–	0.006	–	0.118	0.294	0.42
107/2	0.90	–	–	–	0.011	–	–	–	0.01
108/1	3.86	1.54	14.40	2.06	0.006	–	–	0.160	0.17
108/2	1.41	1.00	1.67	10.39	–	–	–	–	–
108/3	–	–	–	–	–	–	–	–	–
108/4	0.64	–	–	–	0.005	0.124	0.148	0.567	0.84
110/1	–	–	–	–	<0.004	–	0.018	0.003	0.02
112/1	4.50	1.67	19.29	4.89	<0.004	0.666	0.026	0.015	0.71
112/2	1.54	0.90	4.24	2.19	<0.004	–	–	0.004	0.01
112/3	1.29	–	2.06	0.64	0.009	0.145	0.120	0.048	0.37
112/4	–	–	–	–	–	–	–	–	–
114/1	5.66	2.06	19.30	2.83	0.368	0.720	0.099	<0.003	1.19
114/2	0.77	0.51	2.32	0.77	0.131	0.221	0.106	0.010	0.47
114/3	–	0.64	0.39	0.51	–	–	–	–	–
115/1	2.70	–	9.26	1.41	2.340	0.630	0.021	0.018	3.01
115/2	0.64	–	0.39	–	0.928	0.183	0.197	0.136	1.44
115/3	–	–	–	0.26	–	–	–	–	–
115/4	–	–	–	1.67	0.195	0.120	0.071	0.095	0.48
116/1	2.96	0.64	12.86	0.39	2.550	0.783	0.206	2.730	6.27
116/2	0..51	–	57.89	–	0.858	0.172	0.122	0.832	1.98

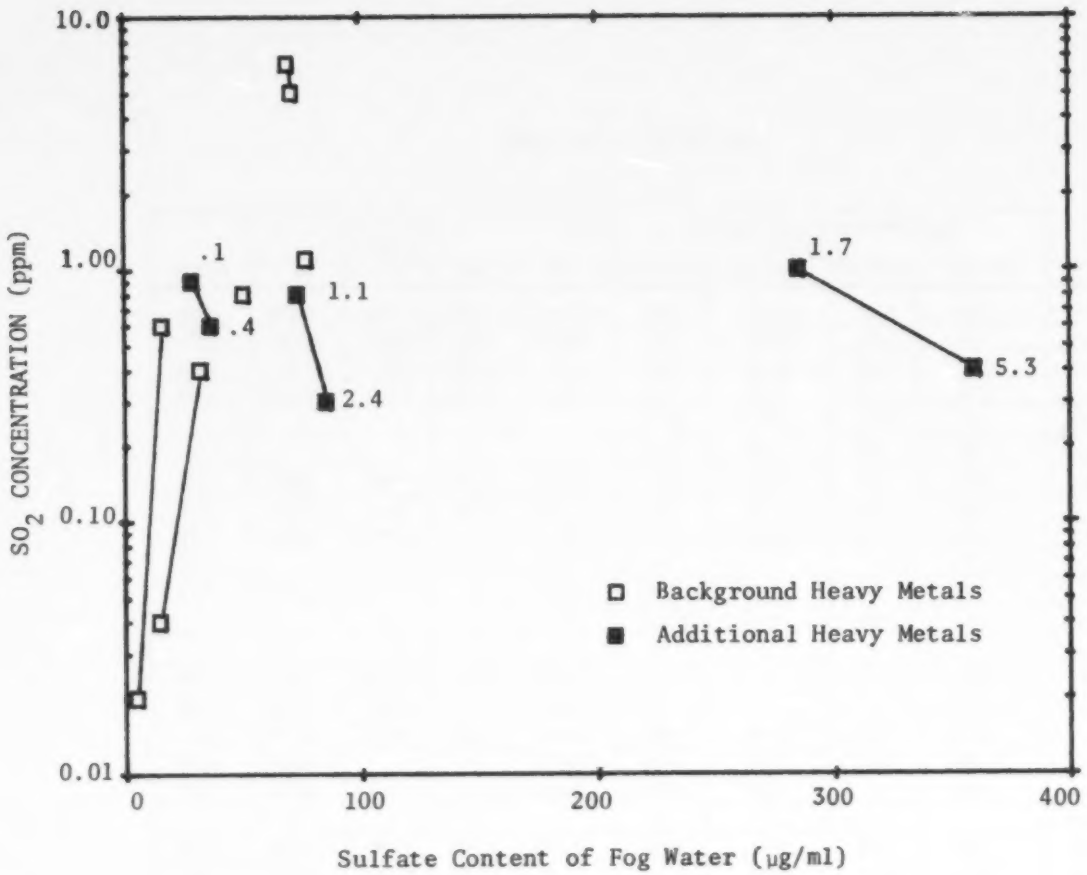

Figure 12 Dependence of Sulfate Content of Fog Water On SO_2 Concentration and Heavy Metals

were not introduced into the chamber, respectively. For those experiments where heavy metals were added (solid symbols), each data point is annotated with the total fog water concentration of Mn and Fe (μg/ml). In addition, the data from two consecutive fogs of a given series are connected by lines in Figure 12. It is clear from this presentation that at trace concentrations of heavy metals (open symbols), sulfate formation in the fog water is correlated with the ambient SO_2 concentration.

The SO_2 concentrations and experimental conditions for the #114, 115 and 116 series of fogs (nonirradiated) were similar to those of the previous fogs with the exception of the type and concentrations of the potentially catalytic heavy metals. Apparently as a result of increasing the concentration of Mn in the #115 series fogs as compared to the #114 series, the sulfate content of the collected fog water increased from about 30 μg/ml (in the #114 fogs) to about 80 μg/ml (for the #115 series of fogs). The #116 series of fogs were essentially a repeat of the #115 series of fogs with the exception that equal quantities of $FeCl_3$ and $MnCl_2$ were added to the nebulizer solution for production of condensation nuclei. The resultant increase in the sulfate content of the fog water of the #116 as compared to the #115 series of fogs points to enhanced catalytic activity within the solution droplets. The level of this increase suggests either that Fe is a much more active catalyst than Mn or, as other investigators have found, that a mixture of Mn and Fe is more active catalytically than would be expected from observing the two in separate tests.

The concentrations of Mn and Fe of approximately 0.01, 1.0, and 5.0 μg/ml found in the collected fog water (Table 12) correspond to atmospheric concentrations of about 0.003, 0.3, and 1.5 $\mu g/m^3$, respectively. The former value approximates the heavy metal concentrations expected in very clean air*, while

*Typical values of Fe and Mn observed at distances of several hundred kilometers off either the eastern or western coasts of the continental United States are about 0.01 $\mu g/m^3$ (Mack, 1978).

typical urban plumes may contain concentrations of heavy metals comparable to the latter values. The data, therefore, suggest that high conversion rates of SO_2 may occur in the atmosphere in the presence of aqueous solution droplets (i.e., clouds or fogs) for concentrations of heavy metals commonly found in urban plumes.

The fact that the sulfate content of the fog water collected from consecutive nonirradiated fogs in each of the series #114, 115, and 116 is virtually constant appears also to be a significant result. This apparent saturation of sulfate concentration implies that further oxidation of SO_2 is inhibited after a specific concentration of sulfate has been reached. As previously cited, this level seems to be dependent upon the concentration of SO_2 and the type and concentration of heavy metals (specifically Mn and Fe). Such behavior is typical of the results found by previous investigators using very different experimental techniques. This saturation effect appears to be related to the dependence of the solubility of SO_2 on the pH of the solution.

The data from the irradiated fogs represent quite a menagerie of SO_2 conversion "rates" (see Table 12). For these experiments, an irradiated fog is defined as a typical fog experiment in which the irradiation system was turned on only for the 25-minute duration of the fog. Inspection of data from individual fogs, however, reveals no systematic increases in sulfate and hence no apparent synergistic effect from the combination of irradiation and fog. For example, while the sulfate content of the collected fog water of irradiated fog #104/1 is slightly higher than that of the similar non-irradiated fogs #100/1 and 101/1, previously observed photooxidation rates for SO_2 ($\sim$0.2% hr^{-1}) in the absence of the fog can explain the difference to within the scatter of the data. A similar statement can be made about the differences between irradiated fog #104/2 and the similar nonirradiated fogs #100/2 and 101/2. The filter samples for the #108 series of irradiated fogs reveal sulfate concentrations which are adequately described by a 0.2% photooxidation of SO_2, providing the sulfate levels are corrected by referencing to Na losses. For the most part, the sulfate contents of the other irradiated fogs fall within the range anticipated by merely adding the expected sulfate from catalytic oxidation and that due to photooxidation of SO_2.

Discussion of Results

One major difference between the results of these experiments and those of previous investigations is the time required for the saturation value of sulfate to form. In the investigations of Junge and Ryan (1958) and Terraglio and Manganelli (1967) periods of about two hours were required before a final sulfate concentration was reached. Barrie and Georgii (1976) found a decreasing rate of SO_2 absorption by 2mm droplets until some three to five hours into the experiment when SO_2 absorption essentially came to a halt. Our fog water data suggest that the final sulfate concentrations have been attained in less time than the 25-minute period of a fog. Since the duration of the fogs was not varied and only one water sample was obtained during each fog, there is not sufficient information to determine precisely how much time was required to reach the final concentration of sulfate in the fog water. The long times required to reach the saturation of sulfate by other investigators suggest that the observed reaction rates may have been influenced by diffusional processes within their solutions for large solution droplets. The catalytic oxidation of SO_2 within the much smaller droplets of the current experiments apparently were not so strongly influenced by diffusional processes within the droplets.

While the oxidation of 5% of the available SO_2 in the one-hour duration of the combined fog and pre-fog haze experiment is an impressive rate, it cannot be interpreted so simply. From data obtained in subsequent portions of each series (i.e., the second and third fogs formed in each air mass) it appears that SO_2 was oxidized until the total sulfate concentration in the solution droplets reached some equilibrium value and there oxidation ceased. This leads us to suspect that the observed total amount of sulfate formed was the upper limit of that which could be produced by catalytic oxidation in each specific air mass. Furthermore, the establishment of equilibrium within the time frame of the experiment suggests that actual oxidation rates in the early portion of exposure may have been greater than the maximum 5% observed.

Fog series #116 shows the greatest formation of sulfate observed in our experiments. The final concentration of about 300 μg/ml of sulfate in the fog water represents an oxidation of about 5% of the available SO_2. It must be recognized that a portion of the sulfate was definitely produced during the dense pre-fog haze and the remainder formed during the fog. While the oxidation of 5% of the available SO_2 in the one hour duration of the combined pre-fog haze and fog experiment is an impressive rate, it appears to represent an upper limit of the catalytic oxidation of SO_2 for this system. The data suggest that even with additional time no further significant amounts of SO_2 would be oxidized. Consequently, for studies of the catalytic oxidation of SO_2 in fogs and hazes the rate of SO_2 oxidation may be less meaningful than the amount of sulfate formed.

In many instances the post-fog sulfate values were unexpectedly lower than the pre-fog or in-fog samples. These losses are probably the result of fallout or sedimentation of fog droplets during the fog event. An estimate of the loss of sulfate occurring during a fog may be obtained by assuming that the loss is proportional to the loss of Na observed during the fog. Referring to Table 12, such losses are generally greater than 50% for the first fog of each series but not quite as large for subsequent fogs of that series. When the sulfate values are corrected by the ratio of the post-fog Na values, most experiments exhibit larger sulfate concentrations, as expected, in the post-fog measurements than in the corrected pre-fog values.

In the case of many of the irradiated fogs, the fallout of fog droplets is reduced due to the fact that heat from the lamps inhibits the growth of the fog droplets. Referring to Table 11 or Appendix A, the mean size of the droplets of irradiated fogs is seen to be smaller than that of the droplets of the nonirradiated fogs. Since the sedimentation velocity is proportional to the square of the radius, the larger fog droplets of the nonirradiated fogs fall out faster than the droplets of the irradiated fogs.

Although the fallout of fog droplets during the fog complicates the interpretations of the experiments, this is precisely the mechanism which is responsible for the major portion of SO_2 scavenging and removal from the

atmosphere. While no effort per se was devoted to investigating the fallout during the fogs of these experiments, future experiments should study this phenomenon.

In summary, the following conclusions concerning the catalytic oxidation of SO_2 for in-fog experiments appear warranted.

1. Analysis of collected fog water reveals sulfate concentrations which appear to be dependent upon SO_2 concentration and type as well as concentrations of heavy metals (specifically Mn and Fe). Sulfate corresponding to the oxidation of more than 5% of the available SO_2 was found in given samples of fog water. This sulfate was produced during some undetermined interval within the one-hour fog and pre-fog haze experiments. The average R_{SO_2} of 5% hr^{-1} may be misleading since there was an apparent saturation in the amount of sulfate formed.

2. There is no obvious synergistic effect on sulfate formation from the simultaneous presence of irradiation and a fog containing only trace concentrations of heavy metals. It appears that the observed rates of photooxidation of SO_2 in irradiated clean air systems ($\sim$0.2% hr^{-1}) are sufficient to describe most increases in the sulfate content of irradiated fogs over those of nonirradiated fogs.

REFERENCES

Anderson, R.J., R.J. Pilié, and J.L. Durham, 1977: "An Evaluation of a Technique for the Improved Collection of Sulfate Aerosols," presented at 51st Colloid and Interface Science Symp., Grand Island, NY, June.

Barrie, L.A., S. Beilke, and H.W. Georgii, 1974: "SO_2 Removal by Cloud and Fog Drops as Affected by Ammonia and Heavy Metals," Proc. Precip. Scavenging Symp., Champaign, IL, U.S. Atomic Energy Commission.

Barrie, L.A., and H.W. Georgii, 1976: "An Experimental Investigation of the Absorption of Sulfur Dioxide by Water Drops Containing Heavy Metal Ions," Atmos. Environ., 10, 743.

Beilke, S., D. Lamb, and J. Muller, 1975: "On the Uncatalyzed Oxidation of Atmospheric SO_2 by Oxygen in Aqueous Systems," Atmos. Environ., 9, 1083.

Byers, R.L., and J.W. Davis, 1970: "Sulfur Dioxide Adsorption and Desorption on Various Filter Media," J. Air Pollut. Control Assoc., 20, 236.

Calvert, J.G. and R.D. McQuigg, 1975: "The Computer Simulation of the Rates and Mechanisms of Photochemical Smog Formation," Int. J. Chem. Kinetics, Symp. No. 1, 113.

Durham, J.L., W.E. Wilson and E.B. Bailey, 1976: "Continuous Measurement of Sulfur in Submicrometric Aerosols," EPA-600/3-088.

Easter, R.C. and P.V. Hobbs, 1974: "The Formation of Sulfates and the Enhancement of Cloud Condensation Nuclei in Clouds," J. Atmos. Sci., 31, 1586.

Fielder, R.S. and C.H. Morgan, 1960: "An Improved Titrimetric Method for Determining Sulfur Trioxide in Flue Gas," Anal. Chem. Acta, 23, 538.

Flocchini, R.G., T.A. Cahill, D.J. Shadoan, S.J. Lange, R.A. Eldred, P.J. Feeney, G.W. Wolfe, D.C. Simmeroth, and J.K. Suder, 1976: "Monitoring California's Aerosols by Size and Elemental Composition," Environ. Sci. Tech., 10, 76.

Georgii, H.W., U. Jendricke, D. Jost, and J. Müller, 1974: "The Distribution of Heavy Metals in Clean and Polluted Atmospheres," Staub 34, 16 (English trans.)

Gerhard, E.R. and H.F. Johnstone, 1955: "Photochemical Oxidation of SO_2 in Air," Ind. Eng. Chem., 47, 972.

Hidy, G.M. and C.S. Burton, 1975: "Atmospheric Aerosol Formation by Chemical Reactions," Int. J. Chem. Kinetics, Symp. No. 1, 509.

Husar, J.D., R.B. Husar, E.S. Macias, W.E. Wilson, J.L. Durham, W.K. Shepherd, and J.A. Anderson, 1976: "Particulate Sulfur Analysis: Application to High Time Resolution Aircraft Sampling in Plumes," Atmos. Envir., 10, 591.

Jiusto, J.E., 1964: Investigation of Warm Fog Properties and Fog Modification Concepts, NASA Contractor Report CR-72.

Johnstone, H.F. and D.R. Coughanowr, 1958: "Absorption of Sulfur Dioxide from Air," Ind. Eng. Chem., 50, 1169.

Junge, C.E. and T.G. Ryan, 1958: "Study of the SO_2 Oxidation in Solution and its Role in Atmospheric Chemistry," Quart. J. Roy, Meteorol. Soc., 84, 46.

Junge, C.E., 1960: "Sulfur in the Atmosphere," J. Geophys. Res., 65, 227.

Kasahara, M. and K. Takahashi, 1976: "Experimental Studies on Aerosol Particle Formation by Sulfur Dioxide," Atmos. Environ., 10, 475.

Kocmond, W.C., D.B. Kittelson, J.Y. Yang, and K.L. Demerjian, 1973: "Determination of the Formation Mechanisms and Composition of Photochemical Aerosols," EPA-650/3-73-002, December.

Kocmond, W.C. and J.Y. Yang, 1975: "A Smog Chamber Study of SO_2 Photooxidation Rates and Aerosol Formation Mechanisms," Calspan Report No. NA-5365-M-3.

Likens, G.E., 1976: "Acid Precipitation," C&EN, Nov. 22, 29.

Low, R.D.H., 1969: "A Generalized Equation for the Solution Effect in Droplet Growth," J. Atmos. Sci., 26, 608.

Mack, E.J. 1978: Private Communication

McKay, H.A.C., 1971: "The Atmospheric Oxidation of Sulfur Dioxide in Water Droplets in Presence of Ammonia," Atmos. Environ., 5, 7.

Miller, J.M. and R.G. DePena, 1972: "Contribution of Scavenged Sulfur Dioxide to the Sulfate Content of Rain Water," J. Geophys. Res., 77, 5905.

Piersen, W.R., R.H. Hammerle, and W.W. Brachaczek, 1976: "Sulfate Formed by Interaction of Sulfur Dioxide with Filters and Aerosol Deposits," Anal. Chem., 48, 1808.

Radke, L.F., 1970: "Field and Laboratory Measurements with an Improved Automatic Cloud Condensation Nucleus Counter," Preprints Conference on Cloud Physics, Fort Collins, Colo., Amer. Meteor. Soc., 7-8.

Richards, J.R., D.L. Fox and P.C. Reist, 1976: "The Influence of Molecular Complexes on the Photooxidation of Sulfur Dioxide," Atmos. Environ., 10, 211.

Scott, W.D. and P.V. Hobbs, 1967: "The Formation of Sulfates in Water Droplets," J. Atmos. Sci., 24, 54.

Stedman, D.H. and H. Niki, 1973: "Photolysis of NO_2 in Air as Measurement Method for Light Intensity, Environ. Sci. Tech., 7, 735.

Terraglio, F.P. and R.M. Manganelli, 1967: "The Absorption of Atmospheric Sulfur Dioxide by Water Solutions," J. Air. Pollot. Control Assoc., 17, 403.

Wood, W.P., A.W. Castlemen, Jr., and I.N. Tang, 1975: "Mechanism of Aerosol Formation from SO_2." J. Aerosol. Sci., 6, 367.

APPENDIX A

MICROPHYSICAL CHARACTERISTICS OF SELECTED LABORATORY FOGS

Included in this Appendix are collections of the characterizations of selected fogs which were produced as a part of the program to investigate the catalytic oxidation of SO_2 in fogs and clouds. Several size distributions of fog droplets are presented for each of the fogs. A legend with each size distribution describes: (1) The age of the fog, T, in minutes; (2) The mean radius of the fog droplets, R, in microns; (3) The total number of fog droplets per cm^3, N; (4) The liquid water content of the fog, W, in grams per cubic meter; and, (5) The visibility in meters, V. All of these values are based upon the measured size distribution of the fog droplets. Located immediately below the legend of each size distribution is the identifying number of the fog. For more information concerning the parameters of each fog, refer to Table 12.

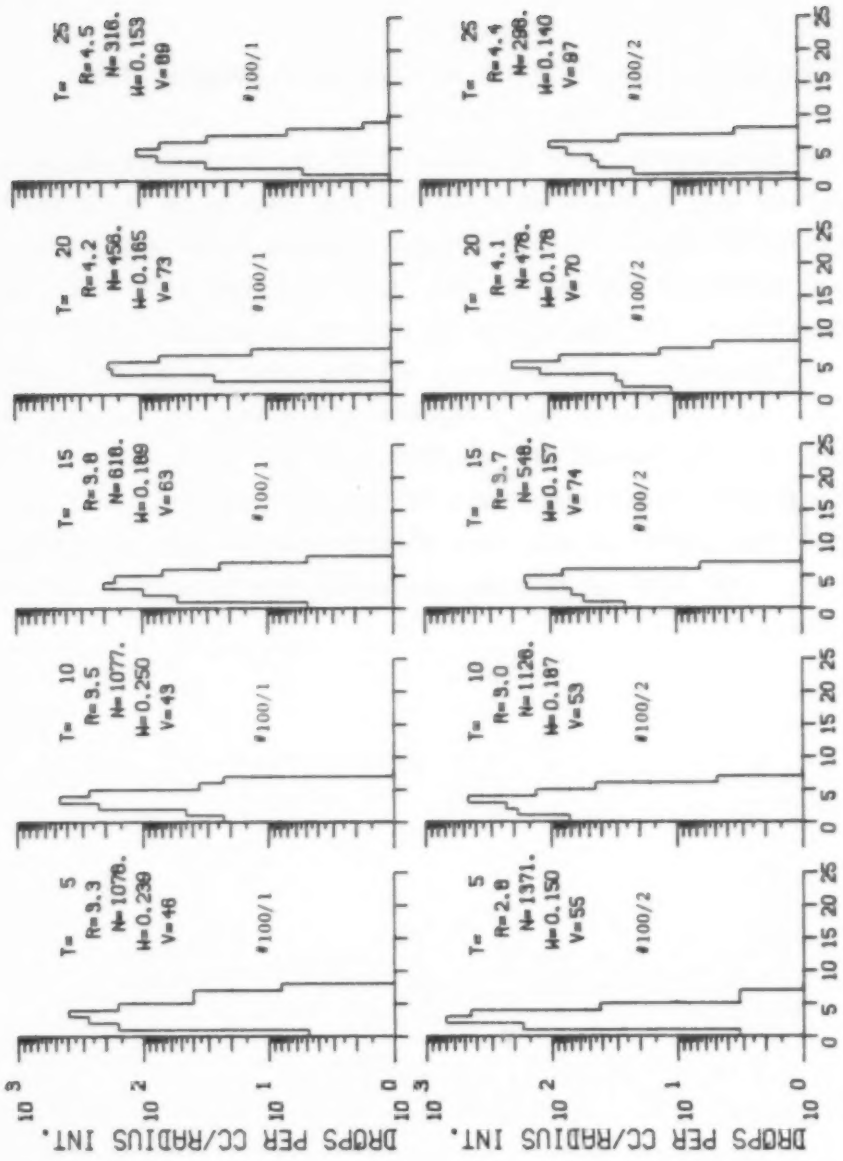
T= 5
R=3.3
N=1076.
W=0.239
V=46
#100/1
T= 10
R=3.5
N=1077.
W=0.250
V=43
#100/1
T= 15
R=3.8
N=618.
W=0.188
V=63
#100/1
T= 20
R=4.2
N=458.
W=0.185
V=73
#100/1
T= 25
R=4.5
N=316.
W=0.153
V=80
#100/1
T= 5
R=2.8
N=1371.
W=0.150
V=55
#100/2
T= 10
R=3.0
N=1120.
W=0.187
V=53
#100/2
T= 15
R=3.7
N=548.
W=0.157
V=74
#100/2
T= 20
R=4.1
N=478.
W=0.178
V=70
#100/2
T= 25
R=4.4
N=298.
W=0.140
V=87
#100/2
DROPS PER CC/RADIUS INT.
RADIUS (MICRONS)

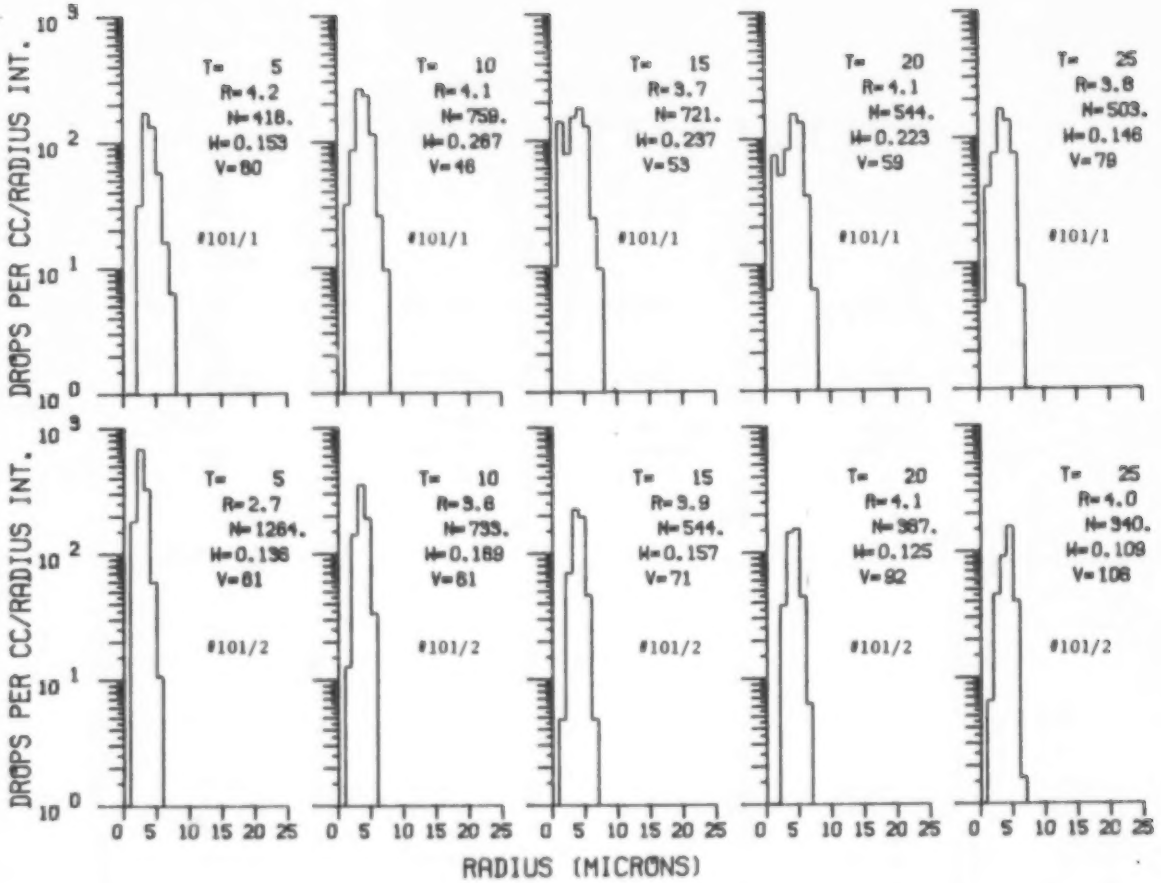
DROPS PER CC/RADIUS INT.
T= 5
R=4.2
N=418.
W=0.153
V=80
#101/1
T= 10
R=4.1
N=759.
W=0.267
V=46
#101/1
T= 15
R=3.7
N=721.
W=0.237
V=53
#101/1
T= 20
R=4.1
N=544.
W=0.223
V=59
#101/1
T= 25
R=3.8
N=503.
W=0.146
V=79
#101/1
DROPS PER CC/RADIUS INT.
T= 5
R=2.7
N=1264.
W=0.138
V=81
#101/2
T= 10
R=3.6
N=733.
W=0.189
V=81
#101/2
T= 15
R=3.9
N=544.
W=0.157
V=71
#101/2
T= 20
R=4.1
N=387.
W=0.125
V=92
#101/2
T= 25
R=4.0
N=340.
W=0.109
V=106
#101/2
RADIUS (MICRONS)

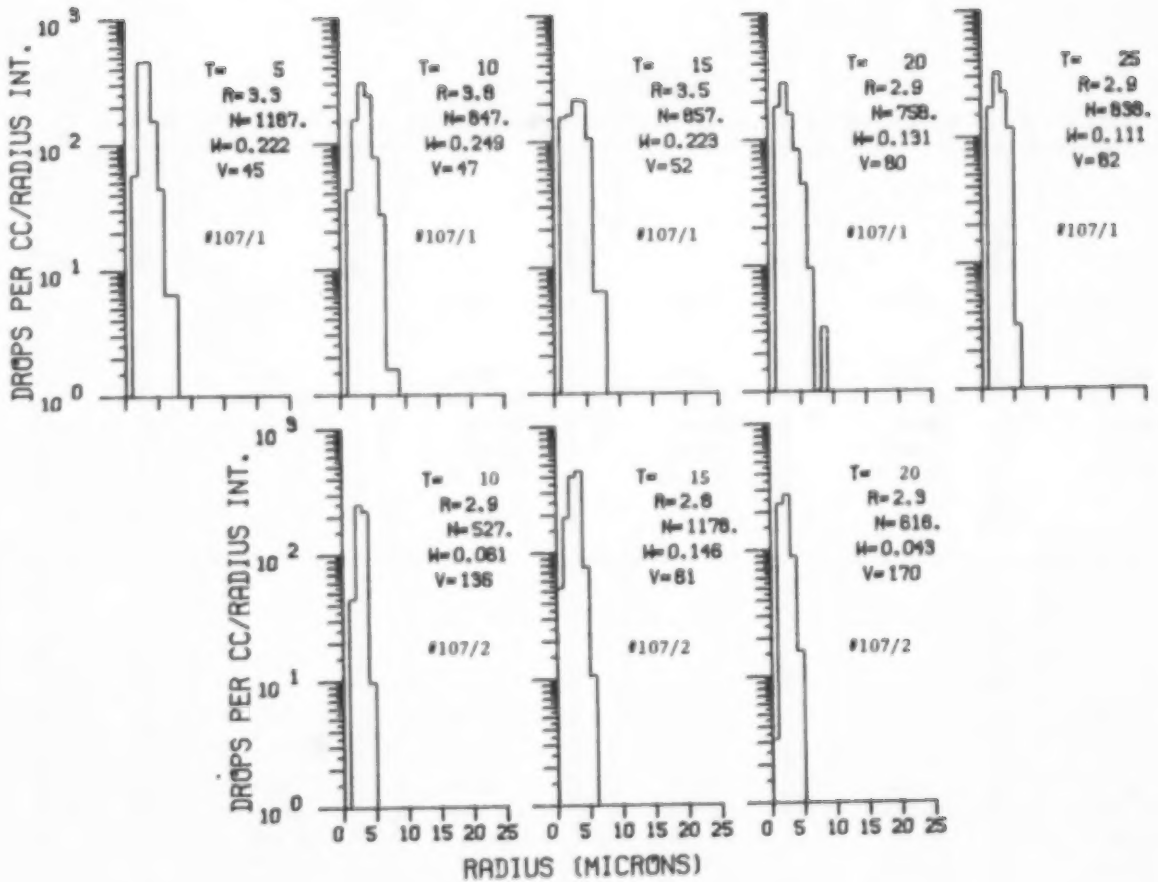
DROPS PER CC/RADIUS INT.
10^3
10^2
10^1
10^0
T= 5
R=3.3
N=1187.
W=0.222
V=45
#107/1
T= 10
R=3.8
N=847.
W=0.249
V=47
#107/1
T= 15
R=3.5
N=857.
W=0.223
V=52
#107/1
T= 20
R=2.9
N=758.
W=0.131
V=80
#107/1
T= 25
R=2.9
N=838.
W=0.111
V=82
#107/1
T= 10
R=2.9
N=527.
W=0.081
V=136
#107/2
T= 15
R=2.8
N=1178.
W=0.146
V=81
#107/2
T= 20
R=2.9
N=818.
W=0.043
V=170
#107/2
0 5 10 15 20 25
RADIUS (MICRONS)

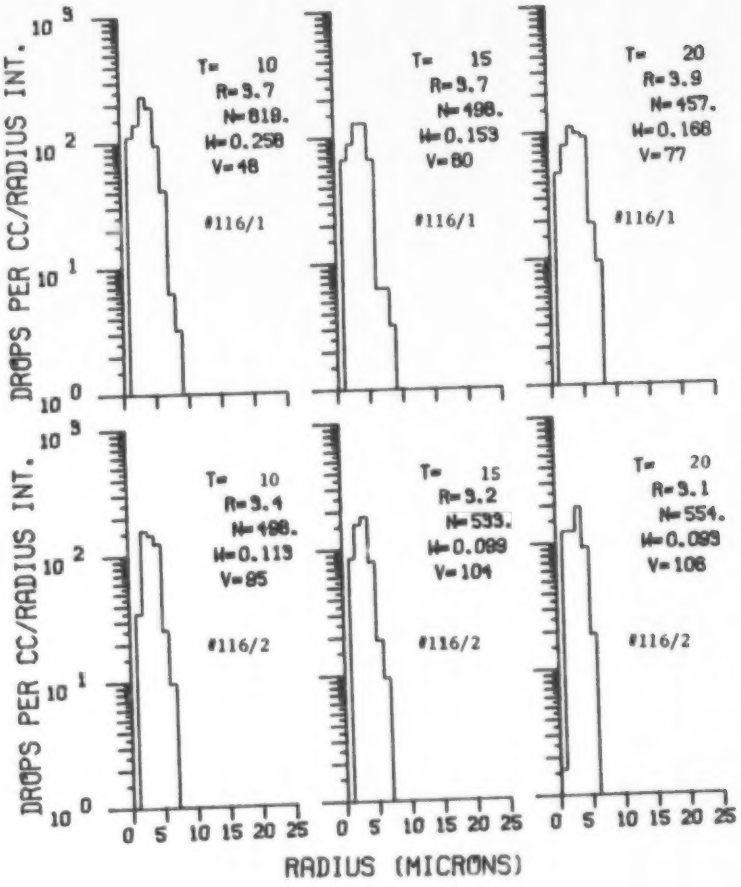
DROPS PER CC/RADIUS INT.
T= 10
R=3.7
N=819.
W=0.258
V=48
#116/1
T= 15
R=3.7
N=498.
W=0.153
V=80
#116/1
T= 20
R=3.9
N=457.
W=0.168
V=77
#116/1
DROPS PER CC/RADIUS INT.
T= 10
R=3.4
N=498.
W=0.113
V=85
#116/2
T= 15
R=3.2
N=533.
W=0.089
V=104
#116/2
T= 20
R=3.1
N=554.
W=0.099
V=108
#116/2
0 5 10 15 20 25
RADIUS (MICRONS)